N72-20680

Technical Status Report

on

Experimental Investigations of a Uranium Plasma Pertinent to a Self Sustaining Plasma Source

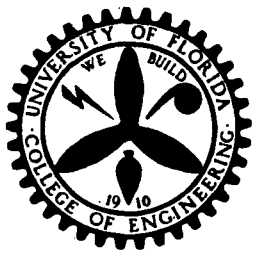

ENGINEERING AND INDUSTRIAL EXPERIMENT STATION

College of Engineering

University of Florida

Gainesville

Technical Status Report

on

Experimental Investigations of a Uranium Plasma Pertinent to a Self Sustaining Plasma Source

by

Richard T. Schneider

Contract NGL 10-005-089

University of Florida

Department of Nuclear Engineering Sciences

Gainesville, Florida

December, 1971

Table of Contents

I. Introduction

II. Uranium Plasma Emission Coefficient in the Visible and Near U.V.

III. Generation of a Uranium Plasma Near Gaseous Core Reactor Conditions

IV. Ballistic Piston Fissioning Plasma Experiment

V. CO_2 Laser Experiment Using Nuclear Reactions as the Ionization Source

VI. Temperature Profile Determination in an Absorbing Plasma

VII. Publications Generated under Grant NGL 10-005-089

I. INTRODUCTION

This research carried out under NASA Grant NGL 10-005-089 is pertinent to the eventual realization of a self-sustained fissioning plasma for applications such as nuclear propulsion, closed cycle MHD power generation using a plasma core reactor, other heat engines such as the nuclear piston engine, as well as the direct conversion of fission energy into optical radiation (Nuclear Pumped Lasers).

Operation of plasma core nuclear reactors for propulsion or other applications requires knowledge of the radiation emitted by uranium plasmas as a function of operating pressures, temperatures, wavelengths, and geometry. The knowledge of partial pressures of the various uranium ionic species and the electrons is mandatory. Criticality calculations, prediction of radiative heat transfer from the gaseous fuel to the working fluid, and design of system startup and control devices require this information.

In order to measure the basic optical radiation properties needed, diagnostic measurement methods and experimental devices simulating plasma core reactor conditions must be developed. The program described herein is aimed toward this goal.

Due to the complexity of the procedures involved in handling the U^{235} isotope, an effort is made to do all research connected with the optical properties of a uranium plasma with natural uranium and to use enriched uranium only for in-core experiments, where the use of U^{235} no longer can be avoided.

The program consists of several experiments, each one being specialized to obtain a certain class of information. These experiments are:

A. Ballistic Piston Compressor (U^{235})

B. High Pressure Uranium Plasma (natural uranium)

C. Sliding Spark Discharge (natural uranium)

D. Fission Fragment Interaction (He^3 and U^{235})

E. Nuclear Pumped Lasers Experiments (He^3 and U^{235})

These individual experiments shall be described briefly.

A. Ballistic Piston Compressor

The ballistic compressor consists of a pressure reservoir, a gun barrel and a high pressure test section. A free traveling piston is accelerated by the high pressure in the pressure reservoir and compresses the test gas into the high pressure test section. Pressures up to 6000 atm and temperatures up to 10,000^{o}K can be reached using helium as test gas. For the experiment in this program a mixture of UF_6 and helium is used. Effective γ, temperature and density of this mixture is determined for a wide range of parameters. The high pressure test section will be subjected to neutron bombardment and the non-equilibrium effects caused by the fission fragment will be investigated. (See also Section IV. Ballistic Fissioning Plasma Experiment).

B. High Pressure Uranium Plasma Experiment

This experiment involves the investigation of optical properties of uranium. A high temperature, high pressure

uranium plasma arc device is used. The arc is contained in a high pressure cell capable of withstanding pressures up to 100 atmospheres. The arc can be operated in two different modes. In one mode a helium cover gas is applied; the other mode is a vacuum arc. In the high pressure mode the emitted line radiation originates primarily from singly-ionized uranium. In case of the vacuum arc, the line radiation observed stems from neutral uranium. Employing different spectroscopic diagnostic techniques, temperatures, particle densities, and emission and absorption coefficients of the uranium plasma for different operating conditions are measured. (See also Section II. Uranium Plasma Emission Coefficient in the Visible and Near U.V.).

C. Sliding Spark Discharge

The goal of this experiment is the generation of uranium ion lines. A capacitor bank is discharged through a capillary. The capillary is formed by a UO_2 sinter body. The sliding spark will evaporate the inner surface of the capillary and subsequently ionize the vapor. The power density is very high due to the constriction of the discharge by the capillary. Therefore multiple ionization is observed. Some of the components of the experiment were given to us by NASA-Langley on a loan basis. (See also Section III. Generation of a Uranium Plasma Near Gaseous Core Reactor Conditions).

D. Fission Fragment Interaction Experiment

This experiment involves a glow discharge in argon, helium or the CO_2 laser gas mixture. In the case of He-gas fill, the

He^3 isotope is used. Under influence of an external neutron flux protons and tritons are generated by the $He^3(n,p)T$ reaction. For other gas fills, the plasma is surrounded by a quartz tube, which is in the inside coated with $U^{235}O_2$. The fission fragments formed close to the surface of the $U^{235}O_2$ layer will escape and interact with the glow discharge in the latter case, while in the first case the high energy protons and tritons will fulfill this function. It is expected that this will result in enhanced ionization. This can be detected by analysis of the I-V curve of the glow discharge. Also, Boltzmann plots of the intensities of the detected spectrum lines can be used to measure deviations of the excited states from a Maxwell-Boltzmann distribution.

E. Nuclear Pumped Laser Experiment

This experiment involves in-core testing of a CO_2 gas laser to demonstrate the feasibility of nuclear enhancement of the laser power output. The He^4 of the laser gas mixture is replaced by the He^3 isotope. The $He^3(n,p)T$ reaction is employed to yield high energy protons and tritons, which may enhance the ionization of the laser gas in direct or indirect ways. Further testing with fission fragments are planned. Also testing with liquid uranium compounds as laser medium are planned. (See also Section V. CO_2 Laser Experiment Using Nuclear Reactions as the Ionization Source).

II. URANIUM PLASMA EMISSION COEFFICIENT IN THE VISIBLE AND NEAR U.V.*

J. M. Mack, Jr., J. L. Usher, R. T. Schneider, and H. D. Campbell
Department of Nuclear Engineering Sciences
University of Florida
Gainesville, Florida

Abstract

Measurements of the specific emission coefficient in the near ultra-violet and visible region of a uranium arc plasma are reported. Spatial unfolding of the intensity profile is used to determine the emission coefficient in the spectral range of 2000 Å to 6000 Å. The uranium partial pressure is estimated to range between .001 and .01 atmosphere, and the corresponding temperature range is 5000 - 10,000°k.

Introduction

To develop the technology necessary for the implementation of gas-core reactors, it is necessary to determine the emission coefficient of uranium plasmas at different temperatures, partial pressures, and wavelengths. This property is fundamental to the design considerations related to criticality studies and radiative heat transfer from the plasma core to the working fluid. The interface conditions which are likely to exist at the core-fluid interface can be simulated with a D.C. uranium arc. Uranium, being one of the most complex elements, does not easily lend itself to a theoretical treatment of the emission coefficient (See References (1) and (2) for the most recent theoretical attempts to describe the uranium atom). Thus, experimental investigations of uranium plasma emission are not only fundamental to gas-core reactor design but also serve to support or deny theoretical treatments.

Average uranium plasma emission coefficients of a D.C. uranium arc have been determined previously[3] with an arc in which the emitted radiation was due primarily to singly-ionized uranium. Uranium emission coefficients due primarily to excited atomic uranium are presented in this paper. These measurements are correlated to temperature and particle density of the plasma.

Uranium Plasma Generation

The uranium plasma is generated within a chamber identical with that of Figure 1, Reference (3). Internally, however, arranged concentrically with the cathode-anode configuration, are several annular water-cooled copper segments (disks). These segments are distributed the length of the cathode and arc column to form a wall-stabilized arc. The arc is also run in low vacuum on the order of 3 Torr. Wall-stabilization and evacuation of the arc chamber greatly enhance arc stability. Power input to the arc is limited to about 1000 watts. The length and diameter of the arc are typically 1 cm and .9 cm, respectively.

The operation of the water-cooled segments in the vicinity of the arc column produces a cooling effect on the arc as a whole. This cooling results in an arc which emits primarily by neutral uranium rather than by singly-ionized uranium. Although singly-ionized uranium lines are found, the atomic uranium lines appear to be the dominant radiation. This is confirmed by the spectral line identification performed with this arc.

Data Acquisition System (DAS)

There are two basic sections of the DAS: (1) that which measures the line profile (density), plasma temperature, and line absorption, and (2) that which measures the arc intensity. The components necessary to measure arc intensity are shown in Figure 1.

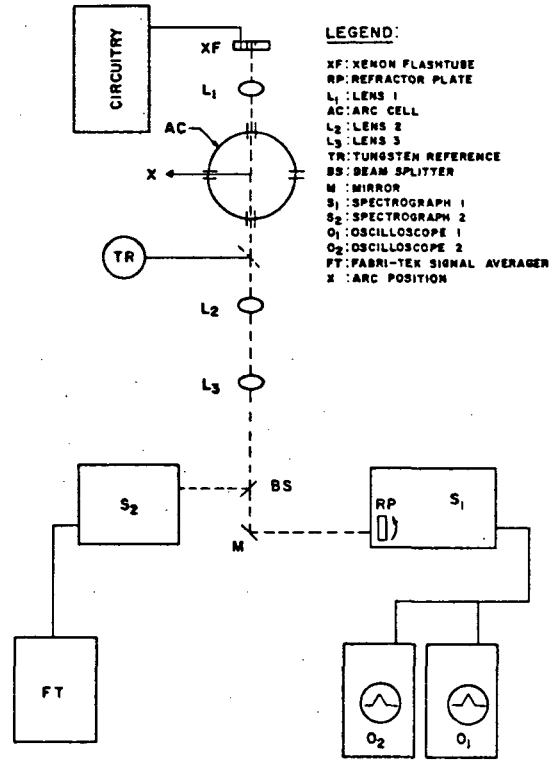

FIGURE 1 DATA ACQUISITION SYSTEM

*This work performed under NASA Grant NGL-10-005-089

A fast-scan spectrograph S2 receives arc light reflected from the front surface of a beam splitter. The phototube response is then monitored and stored digitally by the Fabri-Tek signal-averager. The Fabri-Tek is a time-averaging device which integrates over the small arc fluctuations. This averaging results in very reproductable arc intensity traces as a function of wavelength. Four storage areas on the Fabri-Tek are used for storage of the spectral intensity, $I(\lambda,x)$, where x is a particular position in the arc traverse. Thus, a four point Abel unfolding for spatial resolution of the arc intensities can be performed to obtain the spectral emission coefficient, $\varepsilon(\lambda,r)$, where r is the distance from the arc center. Oscilloscope 02 is used as a Fabri-Tek trigger delay unit which enables the signal-averager to be triggered at any wavelength. The photomultiplier used with S2 is an EMI-9514 with a sodium salicylate window which acts as a wavelength shifter from the ultraviolet to the visible. This serves to expand the phototube system response down to 1900 Å with high sensitivity.

Also shown in Figure 1 are those components necessary for the measurement of temperature, line absorption, and particle density. The beam splitter passes a portion of the arc radiation to S1. A rotating refractor plate (quartz) sweeps a particular line of interest across the exit slit plane of S1. An RCA IP28 phototube placed behind the exit slit responds to the spectral line as it is swept past the exit slit. The resulting line profile is recorded by 01 and 02. At that instant in time when the line is swept to its peak value, a linear Xenon flashtube (EGG FX-12-.25) is triggered (see Figure 2). Timing is accomplished by various electronic delay circuitry. From the oscillogram of 02 is determined the particle density by analysis of the absolute line profile. Oscillograms from 01 allow the determination of line absorption and plasma temperature.

Two tungsten calibration lamps are used to assign absolute units to intensities. One of the lamps is calibrated by the National Bureau of Standards, and its purpose is to periodically cross-check the second lamp which is used in the actual calibration of arc intensities for each arc burn.

Measurement of Plasma Parameters

I. Line Absorption and Temperature

The absorption coefficient of a spectral line is determined by using a background source of constant intensity and measuring the amount it is attenuated as it passes through the plasma. By assuming the nonhomogeneous plasma to be composed of homogeneous rings, an unfolding technique is used to calculate the line absorption coefficient, $\kappa(\lambda)$, from the following equation:

$$\bar{\kappa}(\lambda) = \frac{1}{\ell_{kk}}\left[\tfrac{1}{2}\log_e\left(\frac{V_S}{V_k^T - V_k^P}\right) - \sum_{i=1}^{k}\bar{\kappa}_i\ell_{ki}\right] \qquad (1)$$

where V_S, V_k^T and V_k^P are voltage signals from a photomultiplier tube. The voltages correspond to the background source, the total attenuated intensity, and the plasma intensity, in that order. Figure 2 shows a typical oscillogram of the photomultiplier output.

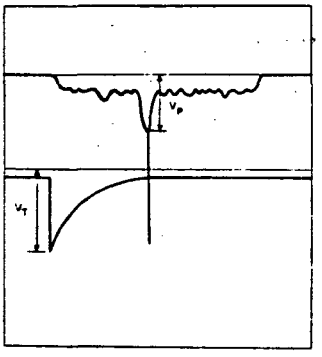

FIGURE 2
OSCILLOGRAM OF PHOTOMULTIPLIER OUTPUT

The background source, in this case a Xenon flashtube, is triggered on the line of interest as shown on the upper trace. The lower trace shows the flash tube signal spread to facilitate measurement of its intensity. The oscillograms are recorded at different chordal positions of the plasma and Equation (1) is used to determine the line-absorption profile. The $\ell_{n,m}$ in Equation (1) represent the length segments in the m^{th} ring along the n^{th} line-of-sight position. Figure 3 is the absorption profile determined for a uranium arc operating with 1000 watts power input.

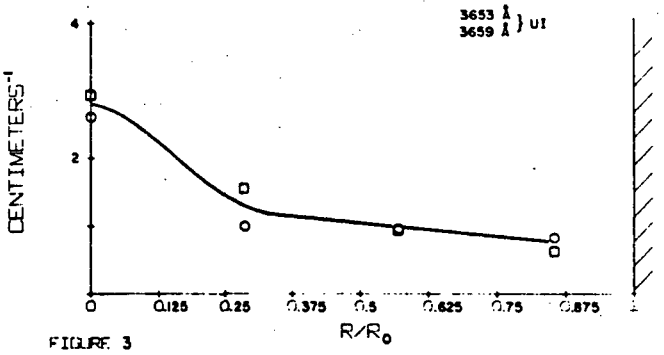

FIGURE 3
LINE ABSORPTION COEFFICIENT PROFILE

The temperature is determined by using an extension of the brightness-emissivity method to the nonhomogeneous case[4]. The technique makes use of the voltages

measured previously as well as the calculated line-absorption values. The temperature method requires that the temperature of the background source be known. The average temperature in the k^{th} ring is determined from the following equation,

$$\bar{T}_k = \frac{C_2}{\lambda} \left\{ \log_e \left[1 + \frac{B_S}{B_k} \left(e^{C_2/\lambda T_b} - 1 \right) \right] \right\}^{-1} \qquad (2)$$

where:

B_S, B_k = the Planck functions representing the intensities of the background source and the k^{th} plasma ring, respectively, at wavelength

T_b = the brightness temperature of the background source

B_k is calculated using the measured voltages and the calculated absorption profile. The complicated expression for B_k is not written here. A uranium temperature profile is displayed graphically in Figure 4 where the power input is 1000 watts.

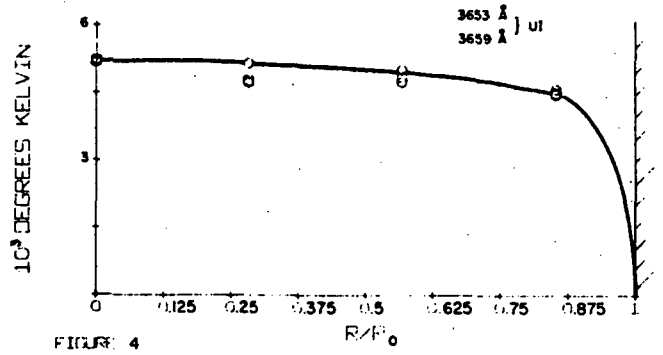

FIGURE 4
U-ARC TEMPERATURE PROFILE

II. Determination of Ul Number Density

The absolute line-intensity method is used to estimate the Ul number density. The general equation for a spectral line is:

$$I \approx \frac{h\nu_{u\ell}}{4\pi} A_{u\ell} N_u S \qquad (3)$$

Utilizing the Boltzmann factor gives the following for the case of negligible ionization:

$$I = \frac{h\nu_{u\ell}}{4\pi} \frac{g_u A_{u\ell}}{U(T)} N_o e^{-E_u/kT} S \qquad (4)$$

where:

u = upper state
I = integrated line intensity in energy per area and time
ℓ = lower state
$A_{u\ell}$ = transition probability in 1/time
h = Planck's constant
$\nu_{u\ell}$ = frequency of emitted photon
N_u = number density of particles in the excited state
N_o = number density of particles in the ground state
U(T) = partition function of the particles in the ground state
g_u = statistical weight of state U
S = plasma depth in cm
kT = thermal energy
E_u = excitation energy

The integrated line intensity of the 3654 Å Ul spectral line is found by sweeping the line across a phototube and recording the response with an oscilloscope (see Figure 2). The same procedure with identical optics is done with an accurately calibrated tungsten strip lamp. The two recorded responses are then compared thus defining the line intensity profile in absolute units. The temperature is determined by the modified brightness-emissivity method, and "$g_u A_{u\ell}$" values are found in (5); U(T) is approximated with the ground state statistical weight.

Solving Equation (4) for N_o for several arc burns at 1000 watts power input results in UI number densities ranging from 10^{15}-10^{16} #/cm³ for the vacuum segmented arc.

III. Determination of Uranium Plasma Emission Coefficient

To determine the emission coefficient it is first necessary to experimentally measure the arc intensity. For the homogeneous case the emission coefficient is found by considering the depth of the plasma. However, the uranium arc is a nonhomogeneous plasma, and so it is necessary to measure the arc intensity at several different line-of-sight positions. Due to the nonhomogeneous nature of the arc, spatial resolution is applied to the intensity to obtain the emission coefficient.

Although some uranium lines have significant absorption, the plasma as a whole will have a small absorption coefficient. Spatial resolution is performed by application of the familiar Abel transform given by Equations (5) and (6) to the measured arc intensities:

$$I(y) = 2 \int_o^X \epsilon(r)\, dx, \qquad (5)$$

and

$$I(y) = 2 \int_y^{r_o} \frac{\epsilon(r)\, r\, dr}{\sqrt{r^2 - y^2}}, \qquad (6)$$

where:

I(y) = intensity from plasma at particular line-of-sight observation,

$\epsilon(r)$ = plasma emission coefficient at chordal locations.

A four-point finite-difference form of Equation (6) is used to transform the measured arc intensities into emission coefficient values at four arc positions. The bandpass of the intensity measurement is approximately 1 A. The resulting calibrated intensities are shown in Figure 5. These intensities are then computer-averaged over a handwidth of 100 A. The results for a power input to the arc of 1000 watts are shown in Figure 6 for 2000-6000 A. The average emission coefficient is shown in Figure 7 for the same conditions. Figure 8 is the center-line intensity of a Helium-uranium arc operated at 15 amperes. The emission coefficients are compared with past results[3] and with theory (1) in Figure 9. Those points with total pressure (P_T) refer to the He-U arc, while those with partial pressure (P_{UI}) refer to the vacuum segment arc.

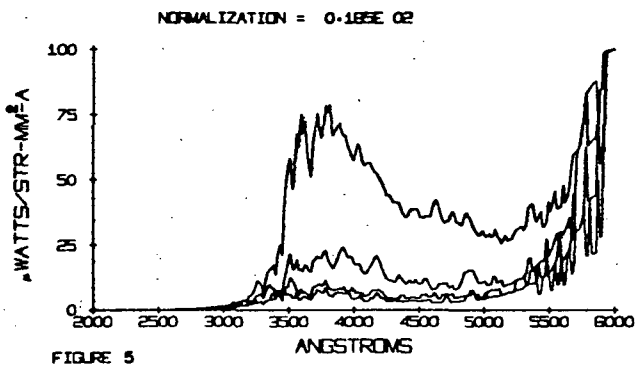

FIGURE 5

URANIUM ARC INTENSITY VS WAVELENGTH

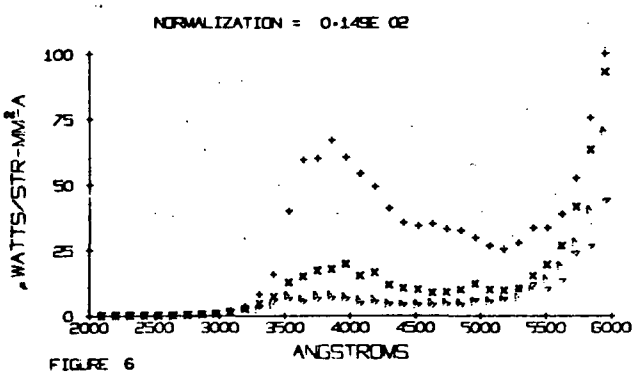

FIGURE 6

AVE. U-ARC INTENSITY VS WAVELENGTH

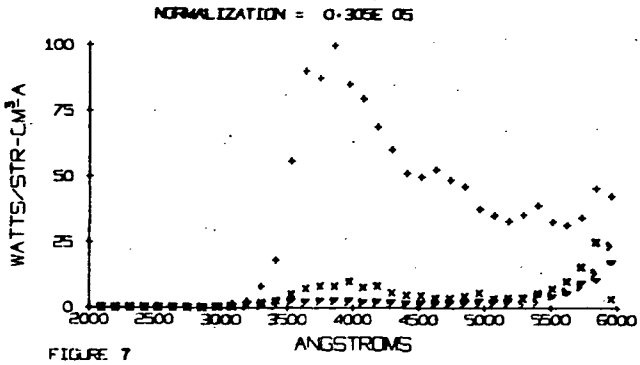

FIGURE 7

AVE. U-ARC EMISSION COEFFICIENT

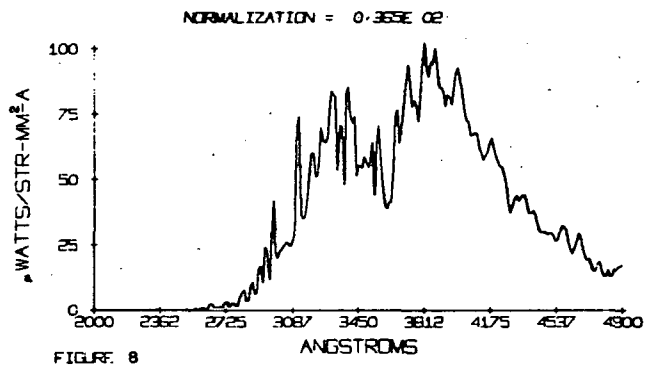

FIGURE 8

HE-URANIUM INTENSITY VS WAVELENGTH

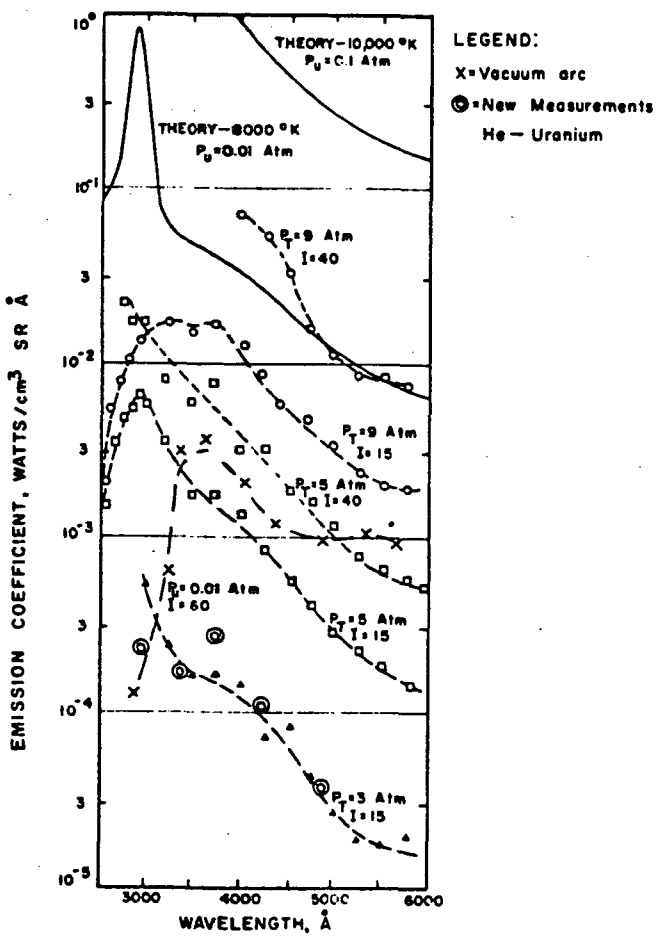

FIGURE 9 COMPARISON OF RESULTS

Concluding Comments

I. Accuracy

The accuracy of measurements of plasma properties is frequently difficult to assess, and this is certainly the case with many uranium plasmas. Of the three plasma properties determined, $-\varepsilon_\lambda$, T, N, certainly the particle density was the most difficult to measure while the emission coefficient was determined with a high degree of certainty.

The temperature measurements by the modified brightness-emissivity method resulted in values somewhat lower than might have been expected. However examination of the spectra revealed that UI was the dominant radiating species rather than UII, as had been the case in earlier work[6]. As explained earlier this lower temperature was attributed to the cooling effect of the water-cooled segments on the arc. It should be mentioned that the validity of the present temperature measurements rests upon the assumption of partial L.T.E. (local thermal equilibrium) down to the lower levels of the transitions studied. It still remains a question as to whether or not the vacuum segmented arc satisfies this condition.

There are three factors which could affect the accuracy of the particle density determination. As in the temperature measurement, it was necessary to assume that L.T.E. conditions prevailed in the plasma. Self-absorption frequently plays an important role in the determination of the total intensity of spectral lines. Fortunately however, the temperature measurement technique used here yields a value of the optical depth which was used to account for this effect. Finally, there is the uncertainty associated with the transition probabilities which had to be used in this measurement.

II. UI Emission

Figure 5 for the UI vacuum arc clearly shows that there is no significant radiation below 3500 Å. On the other hand, the intensity from the higher temperature UII arc (see Figure 8) is strong in the spectral range of 3000-3500 Å. Hence, it is evident that most of the U.V. radiation is generated by ionized uranium.

III. Future Work

It was found that operation of a shorter vacuum arc at 1000 watts resulted in a much more intense uranium plasma. Since the arc column was shorter, the water-cooled segments did not have a significant arc-cooling effect and, thus, the arc became predominantly a UII plasma -- but one with instabilities. Future plans will be to make a longer arc with higher power input to hopefully obtain a very stable UII vacuum arc. Similar measurements to those reported in this paper will be taken on this arc.

Acknowledgements

The authors would like to thank students N.A. Smith, D. Baker, and J. Dixon for their help throughout the year. Special appreciation is in order for the assistance given by K. Fawcett in realizing the complex circuitry necessary for the completion of this experiment. Finally thanks are in order for the help Dr. C. D. Kylstra has given in building the segmented arc.

Bibliography

1. D. E. Parks, G. Lane, J. C. Stewart, and S. Peyton, "Optical Constants of Uranium Plasma," Report GA-8244 (NASA-CR-72348), Gulf General Atomic Incorporated, February, 1968.

2. A. S. Keston and N. L. Krascella, "Theoretical Investigation of Radiant Heat Transfer in the Fuel Region of a Gaseous Nuclear Rocket Engine," Report NASA-CR-695, United Aircraft Corporation, January, 1967.

3. C. D. Kylstra, R. T. Schneider, and H. D. Campbell, "Uranium Plasma Emission Coefficients," AIAA Paper No. 70-692, presented at the AIAA 6th Propulsion Joint Specialist Conference, San Diego, California, June, 1970.

4. J. L. Usher, "Temperature Profile Determination in an Absorbing Plasma," Master's Thesis, University of Florida, August, 1971.

5. C. H. Corliss and W. R. Bozman, "Experimental Transition Probabilities for Spectral Lines of Seventy Elements Derived from the NBS Tables of Spectral Line Intensities," National Bureau of Standards, Monograph 53, Superintendent of Documents, U. S. Government Printing Office, Washington, 1962.

6. H. D. Campbell, R. T. Schneider, and C. D. Kylstra, "Properties of a Uranium Plasma," presented at the Plasma Dynamics Session of the AIAA 8th Aerospace Sciences Meeting, New York, 1970, reprint #70-43.

III. GENERATION OF A URANIUM PLASMA AT NEAR GASEOUS CORE REACTOR CONDITIONS*

J. F. Davis, III, B. G. Schnitzler, and R. T. Schneider
Department of Nuclear Engineering Sciences
University of Florida
Gainesville, Florida

Abstract

A constricted sliding spark discharge is used to generate a high density, high temperature uranium plasma. Uranium particle densities up to 10^{20} cm^{-3} are obtained over a temperature range of 30,000°K - 50,000°K. The device consists of a capillary discharge channel lined with pressed and sintered UO_2. A 250 joule capacitor bank is discharged into the channel, producing a plasma of 10-20 μsec duration. Spectroscopic observations are made over the spectral range of 1300 Å to 2500 Å.

Introduction

The properties of a high temperature uranium plasma are of great interest to many researchers, particularly for development of the Plasma Core Reactor including the Nuclear Light Bulb Engine[1,2,3]. For the latter case, information is needed to determine the amount of radiation emitted at spectral regions where the transparent wall is opaque[4,5]. The operating conditions of a uranium plasma in the plasma core reactor are expected to be in the range of 20,000°K to 40,000°K with pressures of 500-1000 atmospheres. Several experiments have been performed to produce and/or simulate a model uranium plasma at these conditions of high temperature and pressure.

The DC arc has the advantage of producing a plasma that is stable at steady-state conditions [6,7]. Campbell, et al., have produced a stable Helium-Uranium arc at pressures up to 10 atmospheres and temperatures up to 10,000°K[6]. Such operating conditions simulate the properties of the core working fluid interface of a plasma core reactor.

An R-F discharge has also been applied to simulate the conditions in a gaseous core reactor[8,9]. A temperature of up to 7,000°K has been obtained at pressures up to 20 atmospheres.

Another method under development to form a model plasma is piston compression of uranium hexafluoride gas to form a high density plasma[10]. Pressures up to 500 atmospheres of a He-UF_6 mixture have been reported; however the temperature is expected to be of the order of 1000°K.

The sliding spark discharge as described in this paper has a short lifetime and small volume, but has the advantage of producing a high density-high temperature uranium plasma, approaching gaseous core reactor conditions.

The vacuum spark has been found to be an excellent source for studying the spectra of metals in the extreme ultraviolet region. Vodar and Astoin discovered that a high vacuum spark discharge could be produced at lower voltages and with less sputtering of electrode material if the electrodes were separated by, but in good contact with, an insulator[11]. The spark discharge occurs on the surface of the insulator, therefore the name "sliding spark discharge". Many modifications of the sliding spark have been published[12,13,14,15]. The emitted spectrum is characteristic of the electrodes and insulation material. The plasma produced consists of a well defined and relatively long discharge channel. Very high light intensities can be obtained. Spectra with up to 500 eV excitation energies have been observed with a sliding spark.

Description of Apparatus

Conrads has performed considerable work in the area of sliding spark discharge[13,14,16,17]. A similar apparatus is employed in the present experiment with some modifications to introduce the uranium.

The experiment consists of two carbon electrodes held firmly against a high density polyethylene insulator through which a discharge channel is drilled. The carbon electrodes, polyethylene insulator and the uranium insert are illustrated in Figure 1. The uranium insert is composed of UO_2 powder which has been pressed and sintered to form a hard, brittle ceramic of the desired size.

The carbon electrodes are positioned 2 cm apart and the discharge channel is 1.4 to 2 mm in diameter. These dimensions define the plasma volume which is viewed axially through the electrodes as shown in Figure 1.

*This work was performed under NASA Grant NGL 10-005-089.

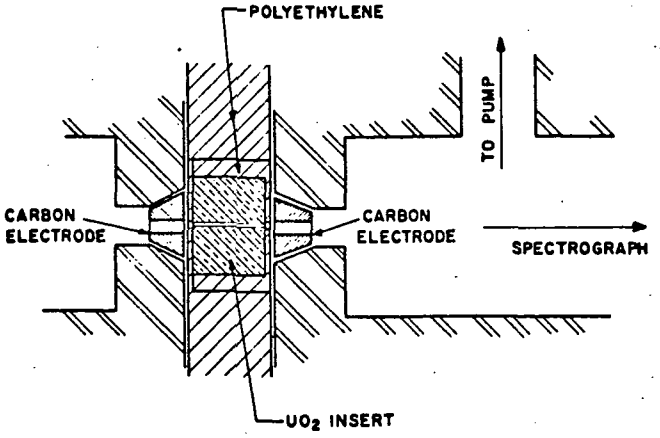

Fig 1. Schematic of Sliding Spark Discharge

A schematic of the circuit is shown in Figure 2. The capacitor bank consists of seven parallel plate capacitors rated at 0.5 μF, 30 kV each. A very low self-inductance of 0.3 nanohenries per capacitor permits a very fast discharge. The bank is connected through a spark gap switch to the electrodes by coaxial cables. The discharge is initiated by triggering the spark gap switch with a 30 kV trigger pulse. After one cycle the spark gap becomes non-conducting breaking the circuit.

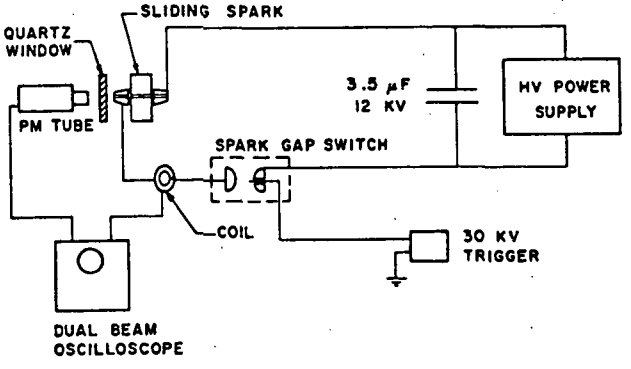

Fig 2. Circuit Diagram

Spectroscopic observations are made with a vacuum spectrograph set on a 1 meter Rowland circle. The spectrograph has a concave grating with 1200 lines/mm yielding a dispersion of about 8 Å/mm. The spectrograph slit and grating are protected from the high velocity particles that ablate off the electrodes and the UO_2 insert by a lithium fluoride window. The lithium fluoride window also separates the two vacuum systems so that the spark pressure can be varied. The short wavelength cutoff of the window is approximately 1200 Å. The film used is Kodak Special Type 101-01.

Description of a Discharge

Typically, the capacitor bank is charged to 12 kv and the residual gas pressure is 100 to 140 microns. The vacuum spectrograph is operated at a pressure of less than 5×10^{-2} microns. The spark discharges the 250 joule bank energy into the capillary channel. After one full cycle (approximately 10 μsec) most of the capacitor bank energy is dissipated. A plot of current and photomultiplier output versus time for a typical shot is shown in Figure 3.

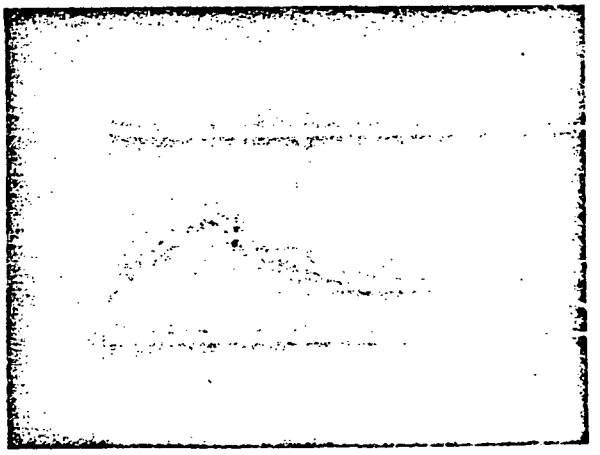

FIG. 3 UPPER TRACE IS CURRENT (20 kA/cm) VS. TIME (20 μsec/cm) LOWER TRACE IS PHOTOMULTIPLIER (10 volts/cm) VS. TIME (20μsec/cm)

The photomultiplier output indicates a plasma duration of approximately 200 μsec. It has not yet been determined if fluorescence of the surrounding insulation and structural materials or a true afterglow causing the long pulse duration.

Results

An estimate of the plasma temperature can be made from the ionization stages present. In the 1500-2500 Å region, the three most intense lines observed were 1548.18 Å (CIV), 1550.71 Å (CIV), and 2296.87 Å (CIII). The plasma temperature can then be approximated by the typical normal temperature of the carbon IV species, 40,000 °K[18].

The maximum pressure produced in the discharge channel is assumed equal to the magnetic pressure. The magnetic pressure, P_{mag}, was calculated from Equation 1.

$$P = \frac{\mu I^2}{8\pi^2 R^2} \qquad (1)$$

With a discharge channel radius of 0.75 mm and a typical peak current of 28 kamp, the magnetic pressure obtained is 220 atmospheres. This pressure corresponds to a particle density of 4×10^{19} cm^{-3} at 40,000 °K.

The capacitor bank discharges with a full cycle time of approximately 10 μsec. The peak plasma temperature is rapidly achieved. Maximum pressure occurs at the maximum current condition. At this instant plasma can then be observed at near plasma core reactor conditions of 40,000 °K and 220 atmospheres.

Complete analysis of the spectra produced involves position and density determinations of a large number of lines. Manual analysis with a measuring microscope requires a prohibitive investment of manpower. The spectrum analysis for this paper was made with the University of Florida Automatic Spectrum Analysis System[19]. The plate was scanned by a Jarrell-Ash scanning densitometer interfaced with an AD-80 analog computer and an IBM-1800 Data Acquisition System. The collected data was processed by programs written at the University of Florida which convert the raw data from the densitometer to transmissions which can be analyzed by the computer. Dispersion relations are automatically calculated from the location of a number of user selected and identified emission lines. Line positions are automatically identified and wavelengths assigned. Transmission plots and lists of lines with corresponding wavelengths are among the available output information.

Plates were scanned at approximately 40 microns/sec and sampled every 4 microns of plate movement. Relative plate position is indicated by a precision linear encoder attached to the plate carriage. Approximately 32,000 positions were sampled while scanning the 1500-2500 Å region.

The 70 mm Kodak Special Film Type 101-01 used has a 5.25 mil thick backing. Because of the thin backing, the film has a tendency to curl away from the film holder under high vacuum conditions. The failure of the film to conform exactly to the Rowland circle introduces irregularities in the calculated dispersion relation. This appears to be the main source of error in wavelength assignment. To minimize these effects, the spectra was analyzed in short segments to which a dispersion relation could be fitted from previously observed uranium lines[20]. The detailed analysis of one such region is presented here.

The transmission plot shown in Figure 4 extends from 2242 Å to 2338 Å. This region was analyzed first because of the abundance of new lines appearing with the addition of uranium to the discharge. In addition, the prominent 2296.87 Å Carbon III line and several known Uranium I lines contained in this region made this spectral region an attractive starting point.

The parameters in the line finding program were selected to locate as many lines as possible automatically. Of the 134 lines located by the program, 16 were eliminated as too weak to be significant or as possible noise. Visual examination of the transmission plots revealed three lines not found by the program. Seven of the remaining lines were identified as carbon and eight as oxygen[21]. Seventy-four previously observed uranium lines were found. Thirty-two lines remain unidentified. A complete listing of these lines and corresponding wavelengths is shown in Table I.

A 50 Angstrom region extending from 1530 to 1580 Å is shown in Figure 5. The prominent emission lines are the 1548.18 Å and 1550.77 Å Carbon IV lines. Also present are Carbon I absorption lines and significant continuum radiation.

The emission spectrum below 2000 Å is of special interest. Addition of uranium to the spark discharge caused significant changes below 2000 Å. A large number of lines were observed which had not been observed in the carbon calibration shots under various conditions. The lack of information on uranium emission below 2000 Å prevents rapid analysis of the obtained spectra.

Since the film integrates the incident light, radiation from the more highly ionized uranium species is extremely weak or can even be obscured by the radiation emitted as the plasma cools.

Conclusions

Uranium emission below the transparent wall material cutoff is significant to the Nuclear Light Bulb design and is also important for radiative power transfer in the coaxial flow plasma core concept. This experiment shows that at near plasma core reactor conditions a complicated spectrum of line radiation exists.

Future work will be directed toward obtaining a comparison between emissions below 2000 Å and at longer wavelengths. A high speed rotating shutter will be used to observe the plasma at peak temperature and pressure in contrast to the present time integrated measurements. A higher pressure discharge can be produced by reducing the diameter of the discharge capillary or by raising the voltage. Higher voltages will also allow lower initial residual gas pressure and thus reduction of impurities. The use

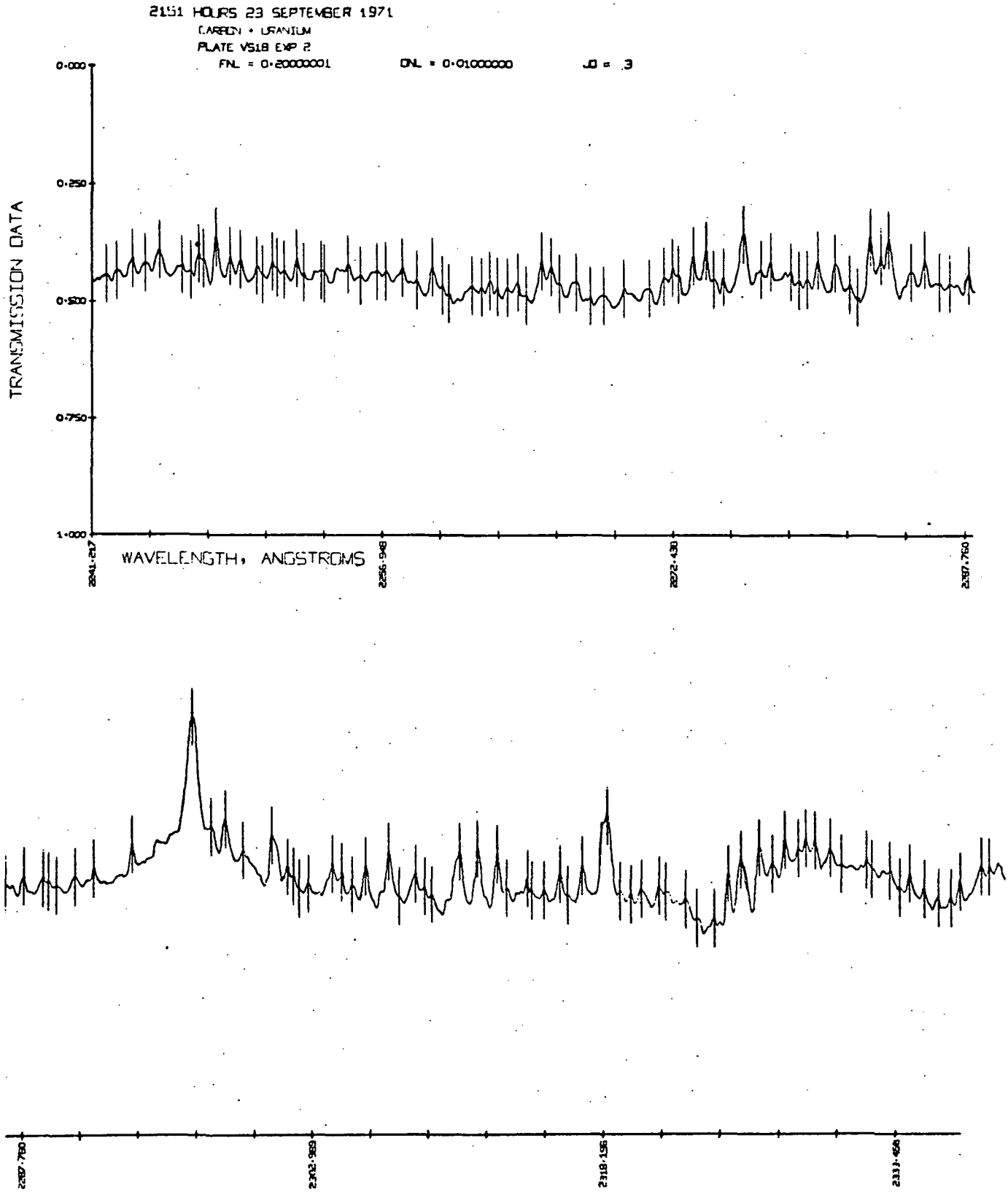

FIGURE 4: TYPICAL CARBON PLUS URANIUM SPECTRA BETWEEN 2242 Å - 2338 Å

TABLE 1: TABLE OF LINES CONTAINED IN FIGURE 4

1	2242.1	C II
2	2242.65	U
3	2243.37	U
4	2244.1	U
5	2244.95	U
6	2246.15	-
7	2246.63	-
8	2247.08	U
9	2247.33	-
10	2248.03	U
11	2248.82	U
12	2249.31	U
13	2250.2	-
14	2250.5	-
15	2251.09	U
16	2251.3	-
17	2251.7	-
18	2252.45	U
19	2252.90	U
20	2255.15	-
21	2255.68	C II
22	2256.19	C II
23	2256.88	-
24	2257.15	-
25	2258.02	U
26	2258.8	-
27	2259.64	U
28	2260.2	-
29	2260.5	-
30	2261.47	U
31	2262.36	U
32	2262.79	U
33	2263.26	U
34	2263.67	-
35	2264.3	U
36	2265.5	-
37	2266.0	-
38	2266.4	-
39	2266.97	U
40	2268.53	U
41	2269.7	C II
42	2270.2	C II
43	2271.81	U
44	2272.4	-
45	2272.68	U
46	2273.36	U
47	2274.2	-
48	2274.47	U
49	2275.12	U
50	2276.05	U
51	2277.02	U
52	2277.98	U
53	2278.63	U
54	2280.14	U
55	2281.0	-
56	2281.84	U
57	2282.78	U
58	2283.34	U
59	2283.72	U
60	2284.83	U
61	2285.66	U
62	2286.4	O III
63	2287.2	O III
64	2287.80	U
65	2288.9	-
66	2289.32	U
67	2289.7	-
68	2290.67	U
69	2291.6	-
70	2293.62	U
71	2296.87	C III
72	2297.72	U
73	2298.37	U
74	2299.2	U
75	2300.89	U
76	2301.51	U
77	2302.0	-
78	2302.69	U
79	2303.93	U
80	2304.4	U
81	2305.65	U
82	2306.91	U
83	2308.7	O III
84	2308.9	U
85	2309.3	U
86	2310.36	U
87	2310.67	U
88	2311.68	O III
89	2312.56	U
90	2313.2	U
91	2314.3	-
92	2314.76	O III
93	2315.52	O III
94	2315.88	U
95	2317.16	U
96	2317.37	O III
97	2318.47	U
98	2319.52	O III
99	2320.2	-
100	2321.1	-
101	2322.5	-
102	2324.03	U
103	2324.8	U
104	2325.46	U
105	2326.45	U
106	2327.2	-
107	2327.88	U
108	2328.52	U
109	2329.89	U
110	2329.46	U
111	2330.22	U
112	2332.1	U
113	2333.3	-
114	2334.3	-
115	2335.1	C IV
116	2335.84	U
117	2336.42	U
118	2336.94	U
119	2338.05	-
120	2338.48	U
121	2338.92	U

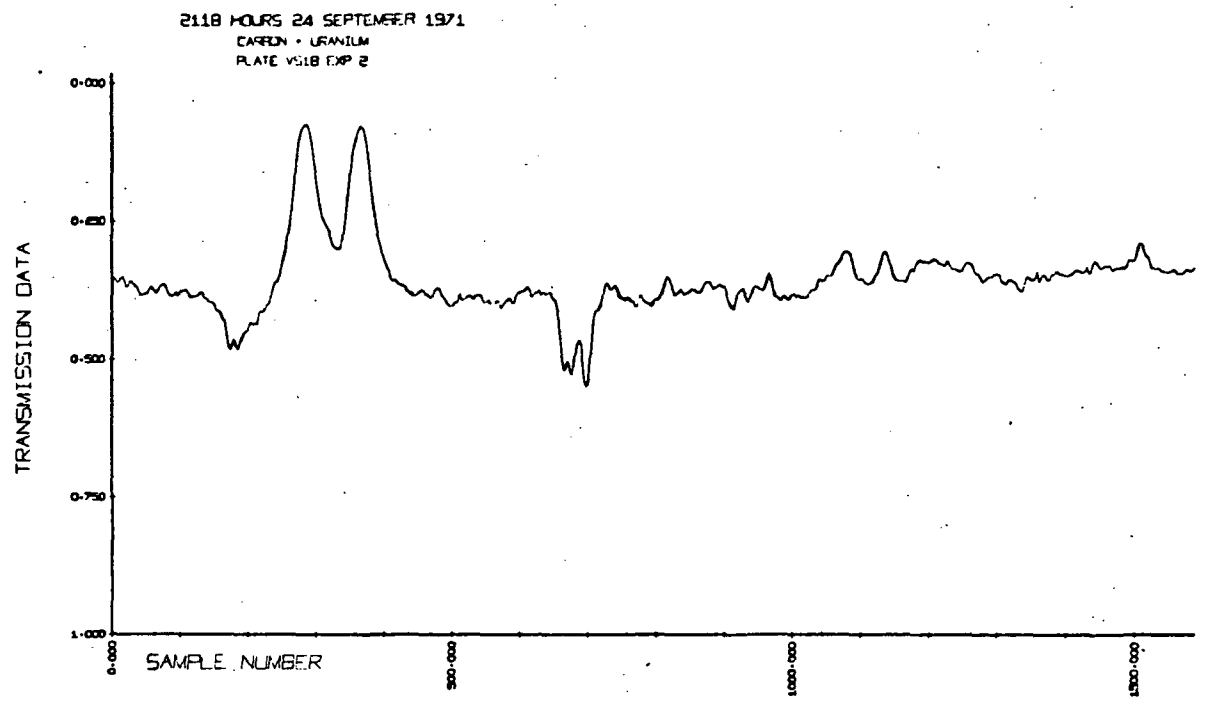

FIGURE 5: TYPICAL CARBON PLUS URANIUM SPECTRA BETWEEN 1530 Å - 1580 Å

of uranium electrodes will eliminate the carbon. An attempt will be made to determine the emission coefficient as a function of wavelength at various pressures.

Acknowledgements

The authors gratefully acknowledge Lou Ayers for his assistance with the computer analysis and Wayne Tuohig for his help in producing the UO_2 inserts.

References

1. J. D. Clement and J. R. Williams, "Gas-Core Reactor Technology," Reactor Technology, Vol. 13, No. 3, Summer 1970.

2. F. E. Rom, "Comments on the Feasibility of Developing Gas Core Nuclear Reactors," Report NASA-TM-X-52644, NASA Lewis Research Center, October 1969.

3. G. A. McLafferty, "Investigation of Gaseous Nuclear Rocket Technology, Summary Technical Report," Report H-9100093-46, United Aircraft Research Lab, November 1969.

4. D. E. Parks, G. Lane, J. C. Stewart and S. Peyton, "Optical Constants of Uranium Plasma," Report GA-8244 (NASA-CR-72348) Gulf General Atomic Incorporated, February 1968.

5. N. L. Krascella, "Theoretical Investigation of the Radiant Emission Spectrum from the Fuel Region of a Nuclear Light Bulb Engine, Report H-9100092-12, UNRL, October 1969.

6. H. D. Campbell, R. T. Schneider and C. D. Kylstra, "Properties of a Uranium Plasma," presented at the Plasma Dynamic Session of the AIAA 8th Aerospace Sciences Meeting, New York, 1970, reprint #70-43.

7. J. M. Mack, J. L. Usher, H. D. Campbell and R. T. Schneider, "Uranium Plasma Emission Coefficient in the Visible and Near UV," paper presented 2nd Symposium on Uranium Plasmas: Research and Applications.

8. W. C. Roman, "Experimental Investigation of a High-Intensity R-F Radiant Energy Source to Simulate the Thermal Environment in a Nuclear Light Bulb Engine," UARL Report J-910900-4, also NASA Contract No. SNPC-70, September 1970.

9. P. J. Marteney, A. E. Mensing and N. L. Krascella, "Experimental Investigations of the Spectral Emission Characteristics of Argon-Tungsten and Argon-Uranium Induction Heated Plasmas, Report G-910092-11, UARL, September 1968.

10. B. E. Miller, R. T. Schneider, K. Thom and G. T. Lalos, "Ballistic Piston Fissioning Plasma Experiment," paper presented 2nd Symposium on Uranium Plasmas: Research and Applications.

11. B. Vodar and N. Astoin, Nature 166, 1029(1950).

12. H. Damany, J. Y. Roucin and N. Damany-Astoin, Appl. Opt. 5 (1966) 297.

13. H. Conrads and H. Hartwig, Z. Angew Phys. 17 (1964) 18.

14. P. Bogen, H. Conrads and D. Rusbüldt, Z. Physik, 186 (1965) 240.

15. G. H. C. Freeman, Proc. Phys. Soc., 86 (1965) 117.

16. H. Conrads, Z. Physik, 200 (1967) 444.

17. H. Conrads, Thesis T. H. Aachen 1966; Berichte der Kernforschungsanlage Jülich Nr. 360.

18. R. H. Fowler and E. A. Milne, Mon Nat Roy Ast Soc 83, 403 (1923); 84, 499 (1924).

19. C. D. Kylstra and R. T. Schneider, "Computerized Spectrum Analysis," Appl. Spec., 24, No. 1, Jan-Feb. 1970.

20. G. R. Harrison, "M.I.T. Wavelength Tables," the M.I.T. Press, 1969 ed.

21. A. R. Striganoy and N. S. Sventitskii, "Tables of Spectral Lines of Neutral and Ionized Lines," IFI/Plenum Data Corporation, 1968.

IV. BALLISTIC PISTON FISSIONING PLASMA EXPERIMENT*

B. E. Miller and R. T. Schneider
University of Florida
Gainesville, Florida

K. Thom
AEC/NASA Space Nuclear Systems Office
U. S. Atomic Energy Commission
Washington, D. C.

G. T. Lalos
Naval Ordnance Laboratory
Washington, D. C.

Abstract

The production of fissioning uranium plasma samples such that the fission fragment stopping distance is less than the dimensions of the plasma is approached by using a ballistic piston device for the compression of UF_6. The experimental apparatus is described. At room temperature the gun can be loaded up to 100 torr UF_6 partial pressure, but at compression a thousand fold increase of pressure can be obtained at a particle density in the order of 10^{19}/ccm. In order to understand the effects of fission fragment interactions, the thermodynamics is studied, for a comparison with subsequent in core measurements involving $^{235}UF_6$.

I. Introduction

A research program has been initiated to investigate the interaction of fission fragments with a uranium plasma. The ultimate goal is a critical fissioning plasma, perhaps preceded by a subcritical assembly.

For such a system a number of conditions have to be fulfilled. The uranium particle density has to be high enough to ensure criticality. Neutron leakage dictates a minimum volume. The temperature should be high enough to create sufficient ionization and excitation to ascertain plasma conditions. These conditions are approached in a device called"ballistic piston compressor"using UF_6 as the gas to be compressed.

Other devices used for uranium plasma research approach the required specifications, but not all at the same time. For example, uranium arcs have high enough temperatures but volume and particle density are too small to allow appreciable nuclear interactions. Arcs are quite useful for optical studies however. King's Furnace type plasmas have the required volume and temperature but the particle density is quite low. They are useful for precision optical measurements, especially measurement of transition probabilities. Pulsed capacitor discharges have high temperature and a high enough particle density. Their volume is too small though. Glow discharges, high or low pressure, have the required volume and temperature. However, a high enough particle density will be hard to achieve.

In the ballistic compressor, the volume and particle density are sizeable and the temperature, although somewhat low, can be improved. It is conceivable that such a device could be built large enough to achieve criticality.

In the present form, the ballistic compressor is a useful research tool to generate information for applications like the gaseous core reactor, the nuclear piston engine (using UF_6 as a working fluid), nuclear pumped lasers and other devices which may depend on the non-equilibrium properties of a uranium plasma or UF_6 seeded plasma.

With its many degrees of internal freedom the UF_6 could exhibit an extremely low ratio of specific heats, γ, such that at heating, no appreciable increase of pressure would occur. Therefore, a first step in this research program is the measurement of the effective γ of UF_6.

II. Ballistic Piston Compressor

The device used for the rapid compression of UF_6 is shown in Figure 1. Since this device is described in detail in References 1, 2, and 3, only a brief description of the compressor and the principle of operation is given.

The compressor consists of five main parts, i.e., the reservoir, piston release section, piston, barrel and high pressure section. The reservoir, which contains the driver gas for the piston, has a volume of 60 liters and was designed for a maximum operating pressure of 136 atmospheres. Sealing this reservoir from the test section prior to firing of the piston is achieved using the plunger arrangement in the piston release section shown in Figure 2. The barrel is approximately 4 meters long with a 50 millimeter bore. Figure 3 shows the high pressure section with its three data

*This work was supported by the National Aeronautics and Space Administration

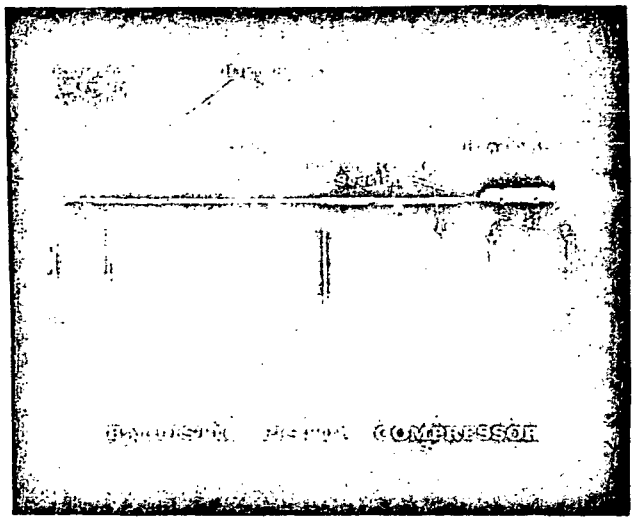

FIG. 1 BALLISTIC PISTON COMPRESSOR

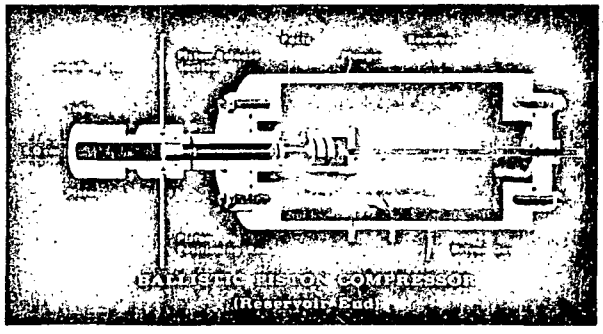

FIG. 2 BALLISTIC PISTON COMPRESSOR (RESERVOIR END)

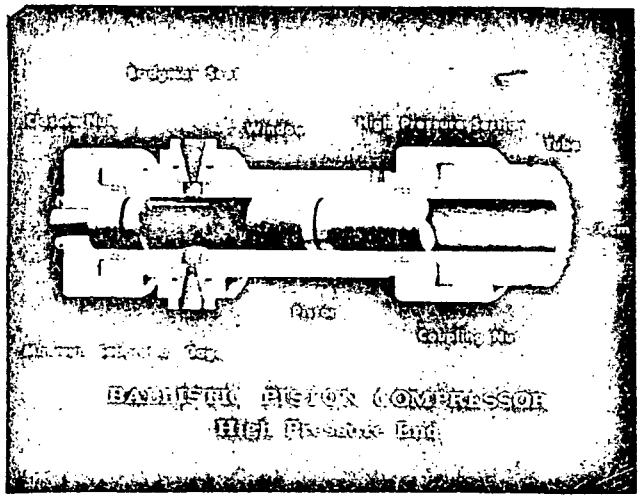

FIG. 3 BALLISTIC PISTON COMPRESSOR (HIGH PRESSURE END)

acquisition ports. This section was designed to accommodate pressures up to 5000 atmospheres. The piston body is made of phosphor-bronze with a molybdenum head for high temperatures and the one used weighs 4 kilograms. Rulon cup seals are attached to the piston to minimize gas leakage between the reservoir and the test section. The entire device is supported with roller bearings beneath the reservoir and high pressure test section to allow for recoil during firing.

Operation of the compressor can best be understood by examining the gas handling system shown in Figure 4. The reservoir is first sealed from the barrel by applying a high pressure, relative to the reservoir pressure,on the plunger to seat it against a teflon gasket. The reservoir is then filled to the desired driving pressure. Next, the piston is seated in the breech by pressurizing the barrel and test section. A vacuum is drawn on both sides of the piston before filling the barrel with the test gas. After filling the test gas, the piston is fired by bleeding the pressure on the plunger to the atmosphere. This causes the reservoir gas to drive the plunger back and the reservoir gas rushes into the breech driving the piston down the barrel.

The high chemical reactivity of UF_6 necessitates additional gas handling system design and construction than that required for most gases. For instance, UF_6 reacts readily with water and because commercial helium is used as the carrier gas for the UF_6 as well as the driver gas, it must be purified by passing it through first an oil scrubber then a cold trap. Sealing the diagnostic ports, the barrel to the test section, and the barrel to the reservoir is also a problem. UF_6 attacks rubber and neoprene, thus viton o-rings with the chemical inertness of teflon and the flexibility of rubber must be used. Another problem is in the type of windows to be used. Both quartz and glass are etched by UF_6 rendering them unsuitable for spectroscopic studies. Sapphire windows have held up quite well and although a film does form on them,it is easily removed. For more details in handling UF_6 see Ref. 5 and 6.

The toxicity of the UF_6 requires a unique gas disposal system. The residual gas after firing is bubbled through a sodium hydroxide solution to remove uranium compounds and any hydrogen fluoride present. Bubbling the gas through an additional solution of potassium iodide removes any free fluorine. The oil in the pumps used for this operation is changed regularly to remove the dissolved uranium compounds. When enriched UF_6 is used, a bellows type compressor and a liquid nitrogen cold trap will be used to reclaim the gas after firings.

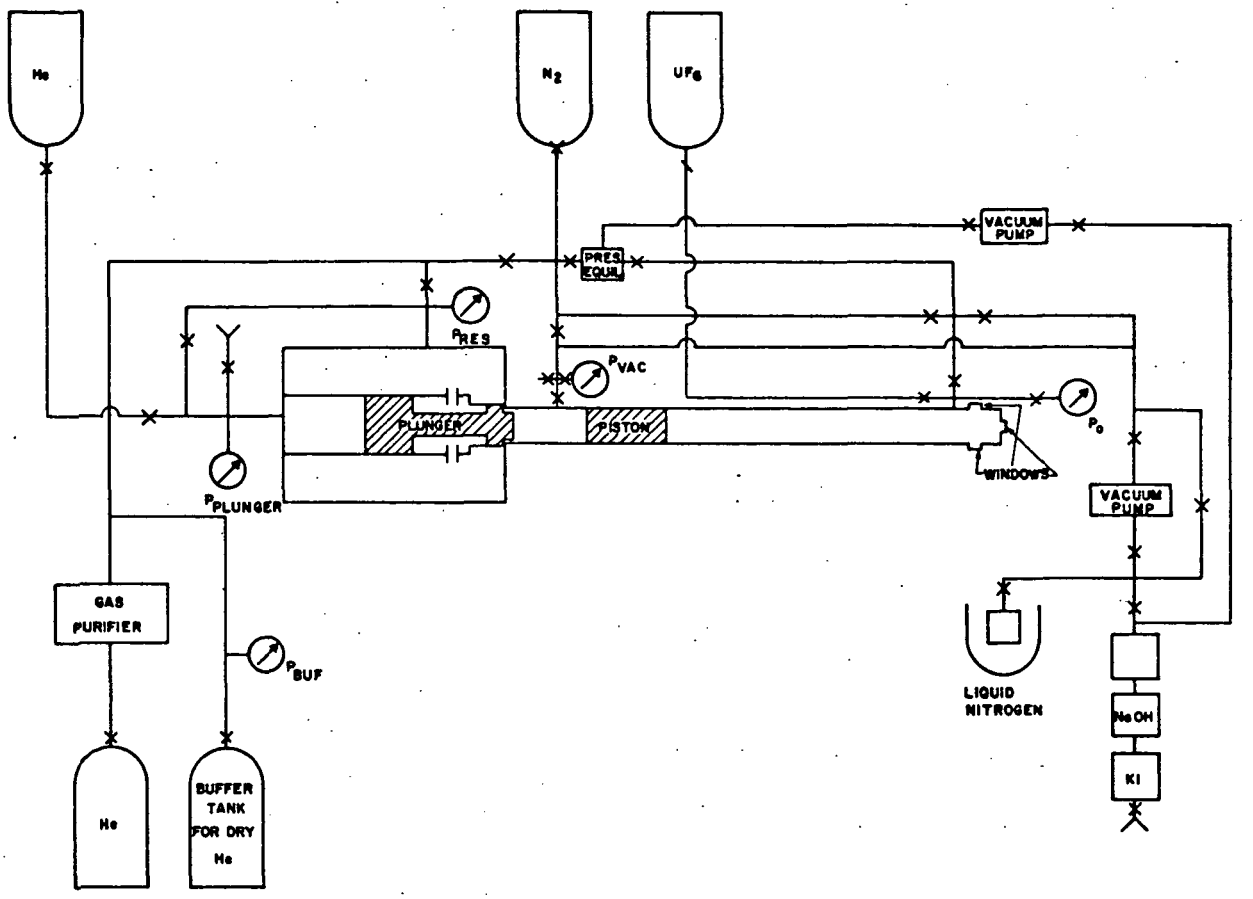

FIG. 4 BALLISTIC COMPRESSOR GAS HANDLING SYSTEM

III. Experimental Techniques

The diagnostic ports in the high Pressure test section are presently being used for pressure and volume measurements at maximum compression. These measurements are being made for pure He and He-UF_6 mixtures to determine the thermodynamics of UF_6 under the rapid compression conditions.

Pressure Measurements

The initial filling pressure of the test section is measured using two Wallace and Tiernan absolute pressure gauges. In all data presented, the UF_6 filling pressure is its vapor pressure at room temperature which is approximately 100 torr. To determine the maximum pressure of the test gas during compression, a high pressure quartz transducer is used in one of the side windows of the test section. This transducer is coupled to a charge amplifier which produces a calibrated output signal that can be read directly in pounds per square inch.

If the reservoir pressure and the test gas initial and maximum pressures are known, an effective isentropic exponent for the test gas can be determined. This is accomplished by equating the work done by the reservoir gas on the piston to the work done by the piston on the test gas. The assumptions made are: (1) ideal test gas, (2) adiabatic process, (3) no gas leakage across piston, and (4) P_{res} = constant.

$$P_{res}(V_o - V) = \frac{P_{max} V - P_o V_o}{\gamma - 1} \qquad (1)$$

where P_o and V_o are initial filling pressure and volume and P_{max} and V are in our case the maximum test gas pressure and the corresponding volume. Rewriting this expression

$$\frac{P_{res}(\gamma-1)}{P_o} = \frac{\frac{P_{max}}{P_o} - \frac{V_o}{V}}{\frac{V_o}{V} - 1} \qquad (2)$$

and substituting the pressure-volume isentropic relation,

$$\frac{P_o}{P_{max}} = \left(\frac{V}{V_o}\right)^{\gamma} \qquad (3)$$

the resultant equation becomes

$$\frac{P_{res}}{P_o}(\gamma-1) = \frac{\frac{P_{max}}{P_o} - \left(\frac{P_{max}}{P_o}\right)^{1/\gamma}}{\left(\frac{P_{max}}{P_o}\right)^{1/\gamma} - 1} \quad (4)$$

If P_{max}/P_o is large and γ is reasonably greater than 1, the second terms in the numerator and denominator of the right side of equation 4 can be dropped. Solving the resultant equation for P_{max} results in

$$P_{max} = (\gamma-1)^{(\gamma/\gamma-1)} P_{res}^{(\gamma/\gamma-1)} P_o^{(-1/\gamma-1)} \quad (5)$$

By rearranging and taking logarithms, this equation becomes

$$\log \frac{P_{max}}{P_o} = \frac{\gamma}{\gamma-1}\left(\log\left(\frac{P_{res}}{P_o}\right) + \log[\gamma-1]\right) \quad (6)$$

A value of γ can then be determined by graphical means. Knowing an effective value for γ gives an indication of the degrees of freedom excited in the compressor test gas (in our case, the UF_6 molecule). The effective value of γ can also be used to give an indication of the temperature at maximum compression if the compression ratio is known. This is done using the isentropic pressure temperature relation,

$$\frac{P_{max}}{P_o} = \left(\frac{T}{T_o}\right)^{(\gamma/\gamma-1)} \quad (7)$$

Volume Measurements

Volume measurements are made using a pin in the test section end plate permitting pressure and volume measurements to be made simultaneously. The piston presses the pin into a cylinder and the pin length remaining outside the cylinder after firing reveals the minimum volume reached.

IV. Results

The results of the measurements of pressure and volume are shown in Figs. 5 and 6. For a given filling pressure a substantially higher maximum compression pressure is reached in UF_6 than in He. Such a behavior is expected according to equation 5 because the expected γ of UF_6 is smaller than that of He. Similarly the volume at maximum compression of UF_6 is smaller than the one of He. In order to determine the effective γ, the compression ratio (P_{max}/P_o) is plotted versus the reservoir to barrel pressure ratio (P_r/P_o) in Figure 7. The slope of the resulting straight lines is related to the effective γ, as can be deduced from eqn. 6. The resulting values for γ are 1.74 for He and 1.59 for He-UF_6 mixtures.

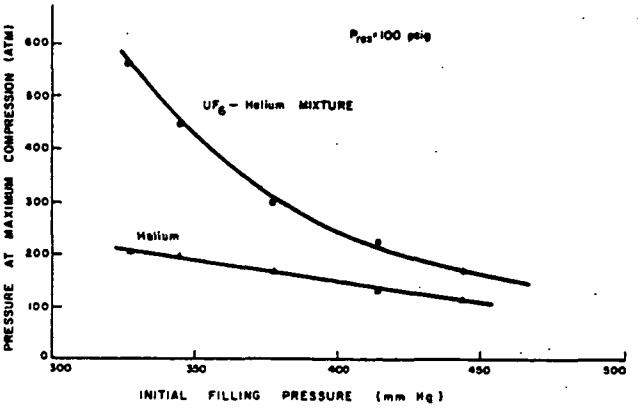

FIG. 5 PRESSURE MEASUREMENTS

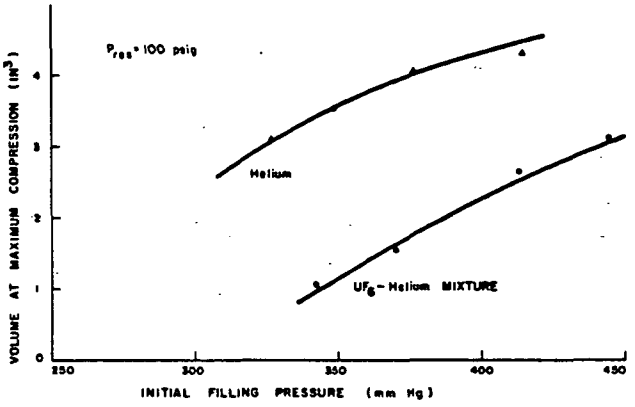

FIG. 6 VOLUME MEASUREMENTS

The smaller effective γ of the He-UF_6 mixture indicates that a large part of the input energy is transferred to the rotational and vibrational degrees of freedom of the UF_6. The effective γ value for pure He is larger than 5/3, due to leakage past the piston during compression.

The temperature of the test gas can be determined using the isentropic pressure-temperature relation (eqn. 7) and the results are shown in Fig. 8. The temperature values for He appear in this graph higher than those of an adiabatically compressed monatomic gas, because of the too large γ for He as deduced from experiment, due to leakage around the piston.

V. Summary

The experimental results show that some but probably not all of the rotational and vibrational levels of UF_6 are excited under rapid compression. This indicates that by compression of He-UF_6 mixtures, temperatures may be achieved, higher than expected for equilibrium conditions.

Limited spectral studies of UF_6 were performed while obtaining the pressure-volume data. The light output

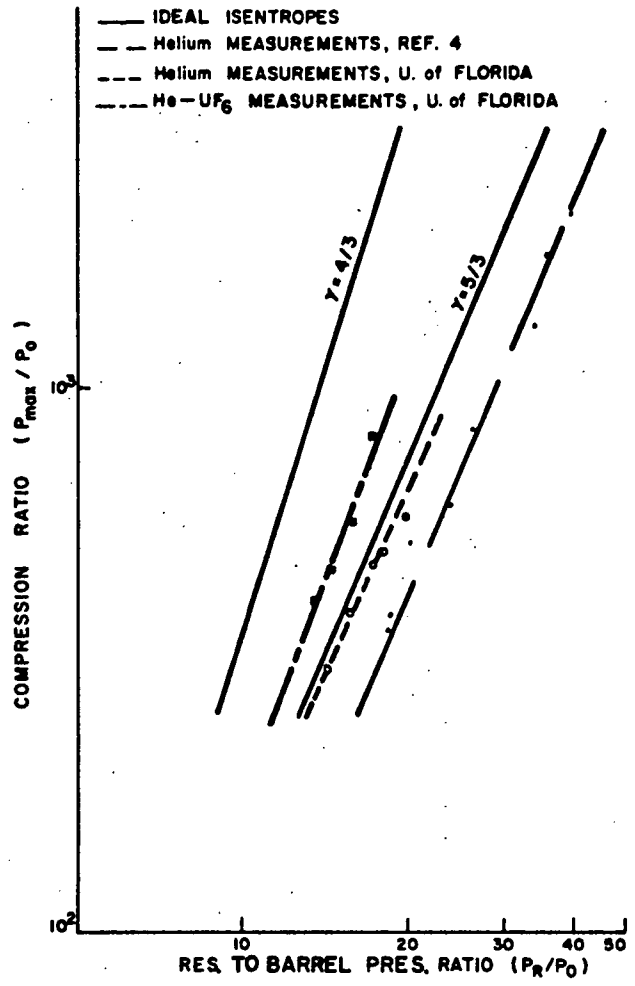

FIG. 7 EFFECTIVE γ DETERMINATION

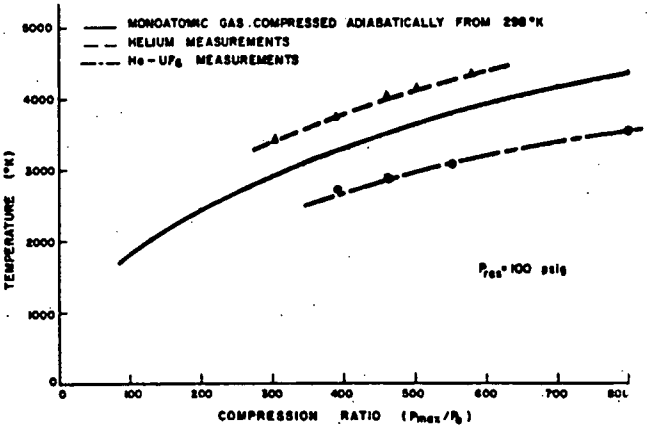

FIG. 8 TEMPERATURE MEASUREMENTS

has been weak due to the minimal compressor conditions used and there has also been a problem with the piston blocking the side windows during compression. These problems are overcome by increasing the test gas filling pressure and the reservoir gas pressure. The amount of UF_6 in the $He-UF_6$ mixture may have to be changed also.

After determining the compressor and test gas conditions required to obtain meaningful UF_6 spectroscopic data and after obtaining such data, the test section will be inserted in the thermal column of the University of Florida Training Reactor. The compressor will be fired with 93% enriched UF_6 with helium as the carrier gas and a comparison will be made of the fissioning UF_6 spectra with the non-fissioning spectra.

VII. Acknowledgements

The authors would like to thank Dr. Richard D. Dresdner for his valuable assistance in the safe handling of uranium hexafluoride.

References

1. Lalos, G. T., NOLTR 63-96, 1963.

2. Lalos, G. T. and Hammond, G. L., NOLTR 66-202, 1967.

3. Lalos, G. T. and Hammond, G. L., NOLTR 70-15, 1969.

4. Hammond, G. L. and Lalos, G. T., NOLTR report in preparation, 1971.

5. DeWitt, R., Uranium Hexafluoride: A Survey of the Physico-Chemical Properties. Goodyear Atomic Corporation. (GAT-280). August 12, 1960.

6. Hudlicky, M., Organic Fluorine Chemistry, Plenum Press, New York, 1971.

V. CO_2 LASER EXPERIMENTS USING NUCLEAR REACTIONS AS THE IONIZATION SOURCE*

H. S. Rhoads and R. T. Schneider
University of Florida
Gainesville, Florida

F. Allario
NASA - Langley
Hampton, Virginia

Abstract

Experimental studies show that the output of a CO_2 laser is significantly increased by products of the nuclear reaction $He^3(n,p)T$.

Helium-3 was used in lieu of the natural helium normally present in the 1:1:8 CO_2:N_2:He laser gas mixture (pressure = 6 torr). The laser assembly was then exposed to a reactor thermal neutron flux of about 10^8 neutrons cm^{-2} sec^{-1}. Power output of the laser doubled while the electrical power input decreased; electrical efficiency was thus more than doubled. Results indicate that additional ionization by the energetic charged particles may be responsible for the improved laser performance.

Introduction

Shortly after the first demonstration of laser action, papers speculating on the possibility of coupling the laser and the nuclear reactor began to appear. The research stimulated by such speculation has begun to show great promise; this paper reports on some aspects of that research.

Motivation

There are many theoretical advantages in pumping lasers directly with energetic nuclear reaction products. The power densities attainable with nuclear reactions are very large compared to those of chemical or electrical processes; an advanced nuclear-powered laser could be quite compact but still immensely powerful.

Such a system could also yield high overall efficiencies. Nuclear-electric power plants might one day operate at 40% efficiency in converting nuclear power to electricity, and the advanced lasers might convert that electrical power to laser light with 25% efficiency (not counting the power requirements of vacuum pumps, compressors and cooling systems). A nuclear laser which converts 10% of nuclear reaction energy to coherent light would thus be quite an attractive prospect.

While the goal of direct nuclear pumping of high-power lasers might be far in the future, nuclear enhancement of electrically-pumped-laser performance as reported in this paper and in other recent publications[1,2,3] are of immediate interest to the industry. A laser whose efficiency is bolstered by nuclear reaction products -- say, alpha particles from a radioactive coating on the walls of a CO_2 laser tube -- would require a smaller power supply and a less robust gas-handling system for a given beam power.

The advantages of compactness and reduced weight would be quite valuable in any airborne or space laser system.

History

Nuclear induced laser action has not been positively reported at this time, though several teams are pursuing that goal[4]. Experiments with solid laser media have not been encouraging, probably due to the degradation of optical quality in crystals and glasses exposed to nuclear radiation. Little nuclear work has been done with liquid laser media.

Gases are not so subject to radiation damage, so that most work has concentrated on gas lasers.

Andriakhin, et al., at the Moscow State University have reported a threefold increase in the power of a CO_2 laser exposed to a beam of protons from an accelerator[1]. The proton beam was used to simulate the products of a nuclear reaction such as $^3He + n \rightarrow {}^1H + {}^3H + 760$ KeV.

This reaction was used in a later experiment in which a Hg-^{3}He gas mixture in a laser tube was exposed to neutrons from a pulsed reactor. The results were ambiguous, but 10 mW peak light pulses were produced[5].

A University of Illinois group directed by G. H. Miley has been active in this field[2,6-8]. Most notable of their recent results is a 20% enhancement in power and efficiency of a pulsed CO_2-N_2-He laser, reported by Ganley, et al.[2] The laser tube was lined with boron-10, which reacts with neutrons to give energetic lithium nuclei and alpha particles. Neutrons were supplied in

*This work was supported by NASA Grant NGL-10-005-089

bursts of 5 x 10^{11} neutrons/cm^2sec peak flux from a pulsed TRIGA reactor.

Experiments with a continuous CO_2 laser have previously been reported by Allario and Schneider[3]. Using a procedure similar to that outlined later in this paper, but with a lower neutron flux, an increase in laser power of a few percent was observed.

Other experimental results are summarized in the survey paper of Thom and Schneider[4].

Experiment

The basic idea of this experiment was to replace the natural helium normally present in the CO_2-N_2-He electrically-pumped laser with helium-3. When the laser was exposed to thermal neutrons in the University of Florida Training Reactor shield tank, the reaction $^3He + {}^1n \rightarrow {}^1H + {}^3H + 760$ KeV altered laser performance.

The laser was a conventional water-cooled internal-mirror design, with a cavity length of 1 m and active discharge length of 66 cm. Tube diameter was 2.5 cm. Mirrors used were a 99% reflective flat and an 85% reflective germanium output coupler with a 10 m radius of curvature. Maximum laser output outside the reactor was about 15 watts with flowing gas, with excitation provided by a DC power supply at (typically) 5 KV and 50 ma. Best performance without gas flow was about 1 watt at 3.8 KV and 30 ma.

The laser assembly and a thermopile for monitoring beam power were enclosed in a watertight aluminum canister and lowered into the UFTR shield tank (a 14-ft. deep tank of deionized water) to a location near the reactor core. Gas, cooling water and electrical power were provided by hoses and cables from outside the shield tank. Thermopile output was monitored with a Keithley millivoltmeter.

Most experimental difficulties arose due to the underwater location of the apparatus. Water leaks were annoying during initial checkouts, and the long vacuum hoses into the tank slowed pumping time. The beam could not be observed directly so that wavelength and resonant modes could not be determined. Mirror alignment could not be optimized after the laser container was sealed; care was required while lowering the assembly into the reactor to avoid shocks that could disturb alignment. Fortunately, radiation problems were not as severe as expected; the optics were apparently not damaged by the neutron, gamma and charged-particle bombardment over several hours of operation. Neutron activation problems were reduced by careful selection of materials, so that overnight "cooling" was usually enough to allow gamma radiation from the apparatus to decay.

The laser could not be operated in the flowing gas mode with helium-3 due to the very high cost ($300 for 2 liters at STP, or $\sim 10^6$ dollars/pound) of the gas. A closed loop system in which the helium-3 could be recycled was considered, but this would permit the buildup of carbon monoxide from CO_2 dissociation and defeat the purpose of the gas flow.

The procedure followed began with evacuating the system and premixing the gases (1:1:8 CO_2:N_2:He) for several minutes in a 2-liter flask to insure uniformity of gas mixtures. With the reactor at the desired power level, the gas mixture was released to the laser system and the DC glow discharge ignited. Current and voltage were monitored on meters and recorders at the power supply panel.

Care was taken to isolate effects due to the helium-3 reaction. Runs were made with natural helium and with helium-3 at zero reactor power; negligible differences in laser output were observed. Some enhancement (about 20%) was seen with natural helium at full reactor power (60 KW, neutron flux $\phi \approx 10^8$ n/cm^2sec), possibly due to the high gamma field near the reactor core (Table 1). The thermopile was not affected by nuclear radiation enough to introduce error. Slight deviations from the desired gas partial pressures and total pressures were found to cause only slight changes (decreases) in laser output.

Results

The effects of nuclear reactions on laser output and efficiency are summarized in Figure 1 and Table 1. In the absence of nuclear reactions, laser output and efficiency improved as discharge current was decreased to the minimum at which a discharge could be maintained (32 ma). With the reactor at full power ($\phi \approx 10^8$ n/cm^2sec), the current could be reduced

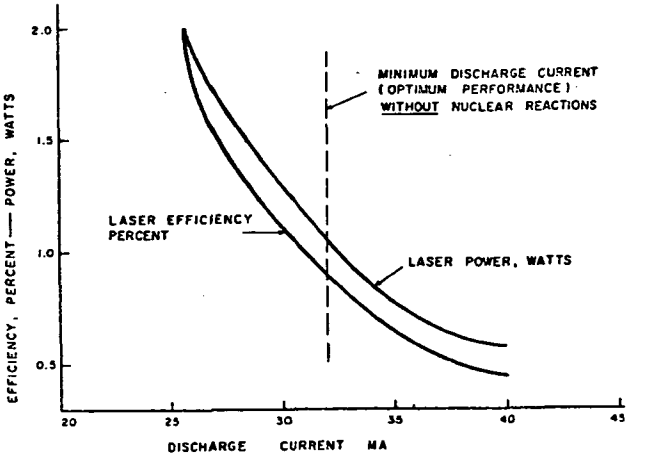

FIGURE 1: EFFECT OF NUCLEAR REACTIONS ON LASER PERFORMANCE.
1:1:8 CO_2:N_2: ^3He, 6 torr

	REACTOR POWER		
CO_2:N_2:He	ZERO	10 KW	60 KW ($\phi = 10^8$)
1:1:8 ^{4}He 6 torr	1.0 W 32 ma 0.86 % efficiency		1.2 W 32 ma 0.97 %
1:1:8 ^{3}He 6 torr	1.05 W 33 ma 0.85 %	1.28 W 27.5 ma 1.18 %	1.95 W 25 ma 1.97 %
1:1:8 ^{3}He + ^{4}He 6 torr	1.0 W 33 ma 0.85 %		1.5 W 29 ma 1.4 %
1:1:8 ^{3}He 14 torr	UNSTABLE DISCHARGE (OVERCURRENT)		0.7 W 46 ma , 5.2 KV 0.3 %

TABLE I : Effects of Nuclear Reactions

still further to about 25 ma with accompanying increase in output to almost twice the original power. Discharge voltage remained approximately constant as the current decreased, so that electrical power input decreased and electrical efficiency went up by a factor of 2.2.

A few runs were made at lower reactor power (10 KW, $\phi \approx 1.7 \times 10^7$ n/cm^{2}sec). In another run at 60 KW, 50% helium-3 and 50% natural helium were used for the helium fraction, giving half the nuclear reactions available with undiluted helium-3. As shown in the table, the enhancement effect was reduced in these runs.

All the above data were taken at a total pressure of 6 torr, which gave a discharge voltage of 3.8 KV. Since one of the great hopes for nuclear lasing is that higher gas pressures might be used, a run at 14 torr was made. Without nuclear enhancement, it was difficult to get the laser discharge to operate at pressures as high as 10 torr. The high current pulse on ignition of the discharge almost always tripped the "overcurrent" protection circuit on the power supply (no load resistor was placed in series with the laser). As the table shows, it was possible with nuclear ionization to achieve laser action in a reasonably well-behaved glow discharge at a pressure 40% above the normal operating limit. Higher pressures than 14 torr were not tried in these experiments, but are planned for a later laser in a higher-flux reactor location.

Some enhancement was observed in 4:1 and 9:1 ^{3}He-CO_2 mixtures, but the output power was quite low (<0.3 W). The power increased perhaps 80% to 100% at full reactor power, but data at such low laser power is not felt to be completely reliable.

Midway through the experimental program described above, a Soviet reference to a laser based on boron trichloride[1] prompted interest in this gas as a possible nuclear laser medium. The $^{10}B(n,\alpha)^7Li$ reaction has been used in other nuclear laser work[2], but never with the boron in gaseous form. Natural boron contains a large fraction of ^{10}B.

Some experiments with BCl_3 were attempted but no useful information was obtained. BCl_3 is highly corrosive and the discharge was run for only a short time before it became evident that a new laser designed to handle such corrosive gases as BCl_3, BF_3 and UF_6 should be built. Such a laser is now being checked out.

Discussion

An estimate of the power P_N being released in nuclear reactions within the laser shows that P_N is quite trivial

compared to the 100-200 watt electrical pump power:

$$P_N = (N_{He}\ \sigma\ \phi)\ Q\ V < 1\ mW$$

N_{He} = number density of ^3He
σ = neutron cross section for ^3He (n,p)T, ~5300 barns
ϕ = neutron flux, $\approx 10^8$ n/cm^{2}sec
Q = energy per reaction, 760 KeV
V = laser volume, $\approx$ 5300 cm^3

However, only a small amount of power is required for the ionization that maintains the discharge[9]. The DC electric field ionizes the gas by providing a number of energetic (>3 eV) electrons, but these energetic electrons are not needed for establishing the population inversion. The N_2 and CO_2 vibrational levels are excited by electron impact at a fraction of an eV, so laser output increases with the density of low-energy electrons. Nuclear reaction products may allow an increase in the number of low-energy electrons by directly producing more electrons in ionizing collision and by relieving the DC power supply of the ionization task so that the electric field strength E may be reduced as fewer high-energy electrons are required.

Perhaps the most important result of nuclear reaction ionization in this laser is the reduction in gas temperature brought about by the lower currents at which the laser would operate. Gas temperature is perhaps the single parameter most important to CO_2 laser efficiency[9].

Nuclear enhancement apparently has an effect similar to the addition of Xe or Cs or other low-ionization-potential atoms to the laser gas: it lowers the effective ionization potential of the laser medium, allowing the electric field (and thus the average electron energy) to be reduced[9]. At higher neutron fluxes, or with the addition of radioactive materials to the walls or gas in the laser, it may be possible to completely relieve the external power supply of the maintenance of the electric discharge and use it solely to accelerate nuclear-generated electrons to the low energies required for molecular vibrational excitation.

Speculation

The properties of such a possible laser system are rather interesting. The production of CO by electron impact ionization would cease since only very few electrons would have the 2.3 eV required to dissociate CO_2. The nuclear reaction products would cause some dissociation, but the net dissociation rate might decrease enough to reduce or eliminate the need for gas flow to remove CO. Catalytic recombination of CO and O_2 back to CO_2 might then be sufficient to give flowing-gas performance in a sealed system.

Another reason for gas flow is the convective removal of heat, particularly in gas dynamic lasers. If the efficiency of a laser can be raised by nuclear effects to the point that more of the electrical power is converted to laser light, less waste energy will need to be removed as heat.

Perhaps most intriguing of all is the fact that high-pressure systems, in which more of the nuclear reaction energy could be absorbed by the gas, probably would show the greatest effects from nuclear enhancement.

The use of a complex, expensive nuclear reactor as a radiation source for nuclear particles is obviously impractical outside the laboratory (unless a way is found to convert fission energy directly to laser light), but it provides a variable source convenient for experiments. Fast ion fluxes equivalent to and greater than those in this experiment are readily available from isotope sources such as polonium-210 once the important processes are understood.

It would be unreasonable to expect optimum performance in nuclear-pumped lasers at the same gas mixtures and pressures found to be best for electric-discharge systems. In particular, Bullis, et al.,[9] report that fractional electron power transfer directly to the upper CO_2 laser level increases with decreasing electron energy, while vibrational excitation of N_2 falls off. Nitrogen is important in discharge lasers where average electron energies are high, but it might be unnecessary or detrimental in a nuclear-ionized laser.

Work in Progress

As previously mentioned, new lasers have been constructed to investigate a wide range of nuclear laser media. Their modular design allows easy interchangeability of components (laser tube, mirrors, Brewster windows and electrodes), giving a significant advantage in flexibility over the laser used in the experiments reported here. The lasers are somewhat more compact to allow investigations in the higher neutron flux of the UFTR thermal column.

In addition to gases such as BCl_3, BF_3 and UF_6 and solid coatings of uranium and boron, the lasers will allow investigations with liquid media. In addition to liquid scintillator solutions, there are a number of uranium-bearing solutions (e.g. of uranyl nitrate, sulfate, fluoride, phosphate and acetate) [12] which fluoresce to some extent and might

exhibit laser action. This is an interesting prospect, since critical reactors of uranium-bearing solutions are well within the grasp of present nuclear engineering technology; this cannot as yet be said for plasma-core reactors.

Summary

Experimental evidence indicates that further nuclear-pumped laser experiments are well worth the experimental difficulties involved. As more data are collected and the physical processes involved become better understood, it is not unreasonable to expect that the goal of direct conversion of nuclear power to coherent light may be realized in the not too distant future.

References

1. Andriakhin, V. M., et al., "Increase of CO_2 Laser Power Under the Influence of a Beam of Fast Protons," JETP Letters, 8, 214-216, 1968.

2. Ganley, T., et al., "Enhancement of CO_2 Laser Power and Efficiency by Neutron Irradiation," Applied Physics Letters, June 15, 1971.

3. Allario, F., and Schneider, R. T., "Enhancement of Laser Output by Nuclear Reactions," NASA SP 236.

4. Thom, K. and Schneider, R. T., "Nuclear Pumped Gas Lasers," AIAA 9th Aerospace Sciences Meeting, January, 1971; AIAA Paper No. 71-110.

5. Andriakhin, V. M., et al., "Radiation of Hg-He^3 Gas Bombarded by a Neutron Stream," ZhETF Pis. Red. 12, No. 2, 83-85, 20 July 1970.

6. Guyot, J. C., et al., "Experiments Using Nuclear Radiation to Pump a He-Ne Laser," Proceedings of Fifth Annual Review of Electronics, University of Illinois, 1967.

7. Miley, G. H. and Verdeyen, J. T., "Advanced Methods for Nuclear Reactor-Gas Laser Coupling," AEC Contract AT(11-1)-2007.

8. Guyot, J. C., et al., "On Gas Laser Pumping via Nuclear Radiations," Symposium on Research on Uranium Plasmas and Their Technological Applications, Gainesville, Florida, January 1970, NASA SP-236 (Supt. of Documents, U. S. Gov't Printing Office $3.75).

9. Bullis, R. H. et al., "Physics of CO_2 Electric Discharge Lasers," Proceedings of AIAA 9th Aerospace Sciences Meeting, January, 1971; AIAA paper No. 71-64.

10. Wiegand, W. J., et al., "Carbon Monoxide Formation in CO_2 Lasers", Appl.Phys.Lett. 16:6,237-9, 15 Mar 70.

11. Karlov, N. V., et al., "Laser Based on Boron Trichloride," JETP Vol. 8 #1 (ZhETF Pis. Red. 8, 22-25, 5 July 1968).

12. Burris, L., "Chemistry and Chemical Engineering" in Etherington (editor), Nuclear Engineering Handbook (New York, 1958; McGraw-Hill), section #11-37.

VI. TEMPERATURE PROFILE DETERMINATION IN AN ABSORBING PLASMA*

J. L. Usher and H. D. Campbell

A method is available for temperature profile determination in the optically-non-thin case which requires only knowledge of the line absorption coefficient of the plasma. It is known as the brightness-emissivity method[1,2] (BEM) and is essentially a line-reversal technique. The two stringent prerequisites for this technique are[3] (a) partial local thermodynamic equilibrium (LTE) down to the lower level of the transition in question, and (b) homogeneity of the plasma. As this diagnostic technique is independent of the atomic properties of the plasma constituents, it can be very useful in plasmas composed of constituents having large atomic numbers. This is so because there is frequently a serious shortage of available and accurate data on the atomic properties of elements with high atomic numbers, e.g., uranium.

The spectral intensity, I_λ^P, emitted by a homogeneous layer of plasma may be expressed as[4]

$$I_\lambda^P = S_\lambda \left\{ 1 - \exp(-\tau_\lambda) \right\}, \qquad (1)$$

where τ_λ is the optical depth of the plasma layer and

S_λ is the source function. The requirement of partial LTE allows one to replace the source function by the Planck function, $B_\lambda(T_e)$, where T_e is the electron temperature of the plasma layer.

If one considers a non-homogeneous plasma to be comprised of concentric rings of homogeneous plasma (Fig. 1), prerequisite (b) above may effectively be removed in the following manner. By placing a standard light source of known intensity behind the plasma, one may calculate the optical depth of the j^{th} line-of-sight position for the plasma from the following expression for the total intensity:

$$I_j^T(\lambda) = I_\lambda^S \exp(-\tau_j(\lambda)) + I_j^P(\lambda), \qquad (2)$$

where I_λ^S is the intensity of the background source as determined previously, and $I_j^P(\lambda)$ is the plasma intensity (at the j^{th} position), which also has to be independently determined. The optical depth along the j^{th} line-of-sight position, $\tau_j(\lambda)$, can be determined directly from Equation (2), and it may also be expressed as

$$\tau_j(\lambda) = 2\sum_{k=1}^{j} \bar{K}_k(\lambda)\, \ell_{jk} . \qquad (3)$$

One makes measurements of τ_j at several line-of-sight positions (Fig. 1) and then computes the average absorption coefficient for the k^{th} ring, $\bar{\kappa}_k(\lambda)$, from the following

expression:

$$\bar{K}_k(\lambda) = \frac{1}{\ell_{kk}}\left[\frac{1}{2}\log_e\left(\frac{B_\lambda^S}{I_k^T(\lambda) - I_k^P(\lambda)}\right) - \sum_{i=1}^{k-1}\bar{K}_i(\lambda)\ell_{ki}\right] \tag{4}$$

Equation (4) is obtained directly from Equations (2) and (3). The ℓ_{jk} term in Equations (3) and (4) represents the chordal length segment present in the k^{th} concentric ring along the j^{th} line-of-sight position. It has also been assumed that the intensity of the background source may be represented by $B_\lambda^S(T_B)$, where T_B is the brightness temperature.

This representation of the background source intensity is chosen to simplify the mathematical calculations; it is not necessary. The choice of sufficiently bright sources may pose problems in the case of optically thick plasmas.

One now proceeds to calculate the average temperature, $\bar{T}_k$, of the k^{th} concentric ring. A combination of Equations (1) and (4) produces the following value for the Planck function, $B_k^P(\lambda, \bar{T}_k)$, of the k^{th} ring:

$$\begin{aligned} B_k^P = \frac{\exp\left[\sum_{i=1}^{k-1}\bar{K}_i\ell_{ki}\right]}{1 - \exp\left[-2\bar{K}_k\ell_{kk}\right]}\Bigg\{ & I_k^T(\lambda) - B_\lambda^S\exp\left[-2\sum_{i=1}^{k}\bar{K}_i\ell_{ki}\right] \\ & - \sum_{i=1}^{k-1}B_i^P\left(1-\exp\left[-\bar{K}_i\ell_{ki}\right]\right)\left(\exp\left[-\sum_{j=1}^{i-1}\bar{K}_j\ell_{kj}\right]\right) \\ & \times\left(1+\exp\left[-2\sum_{j=i+1}^{k}\bar{K}_j\ell_{kj} - \bar{K}_i\ell_{ki}\right]\right)\Bigg\} \end{aligned} \tag{5}$$

The average temperature for the ring is now determined from the inversion of the above Planck function:

$$T_k = \frac{c_2/\lambda}{\log_e\left[\frac{c_1}{\lambda^5 B_\lambda^r} + 1\right]} \qquad (6)$$

Once one has obtained values for κ_λ and T profiles in the plasma, it is also possible to calculate values for the emission coefficient, ε_λ. One makes use of the LTE approximation (Kirchoff's law):

$$B_\lambda = \varepsilon_\lambda / \kappa_\lambda \qquad (7)$$

Previous work[5, 6, 7] in determining the temperature profiles of optically-non-thin plasmas has made use of Equation (7) to determine T(r) and thus requires the determination of both the κ_λ and ε_λ profiles of the plasma; however, the present method requires only the κ_λ profile. It should be noted here that the same experimental data is necessary for both methods. The use of the double-path method by Birkeland and Braun[7] represents an excellent solution to the problem of matching intensities of the plasma and background source. A sensitivity analysis has verified that the errors in the determination of these profiles propagate in a manner similar to those in Abel inversion techniques. Hence more accurate temperature profiles can be determined with the BEM unfolding technique, which only requires the κ_λ profile.

REFERENCES

1. E. M. REEVES and W. H. PARKINSON, "Temperature Measurements for Shock Heated Powdered Solids", Scientific Report No. 1, Harvard College Observatory.

2. W. LOCHTE-HOLTGREVEN, "Plasma Diagnostics", North-Holland, Amsterdam, John Wiley and Sons, Inc., New York (1968).

3. H. R. GRIEM, "Plasma Spectroscopy", McGraw-Hill, New York (1964).

4. S. CHANDRASEKHAR, "Radiative Transfer", Dover Publications, Inc., New York (1960).

5. W. G. BRAUN, Rev. Sci. Instr., 36, No. 6, 802 (1965).

6. P. ELDER, T. JERRICK and J. W. BIRKELAND, Appl. Optics, 4, 589 (1965).

7. J. W. BIRKELAND and W. G. BRAUN, "The Temperature Distribution in a Vortex-Cooled Hydrogen Arc", Paper Presented at the Seventh International Conference on Phenomena in Ionized Gases, Belgrad (1965).

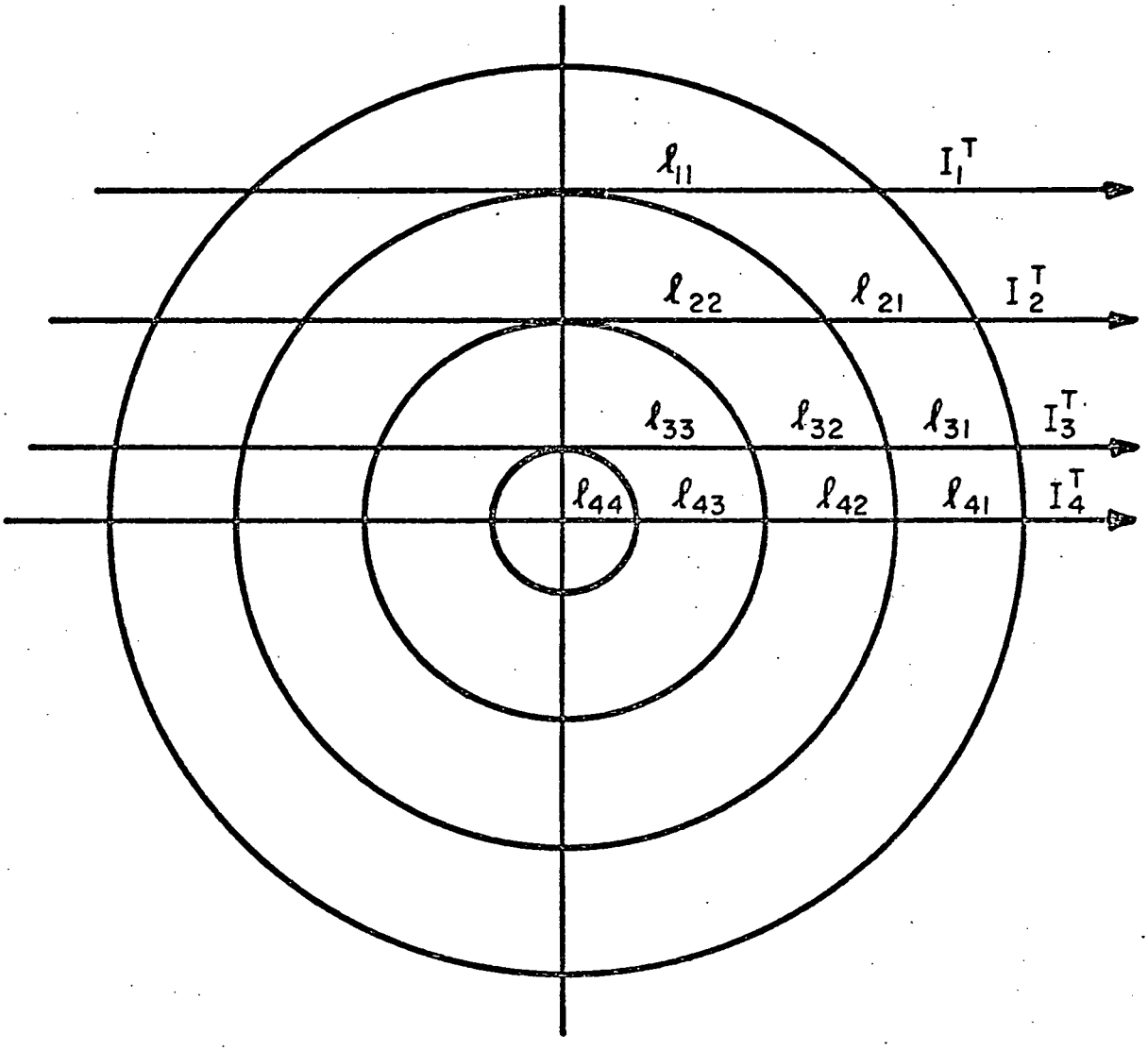

Fig. 1 Ring Division of a Cylindrically Symmetric Plasma

Nomenclature

B_λ	-	Planck function
$B_\lambda^S(T_B)$	-	Planck function representation of background source intensity, T_B is brightness temperature
$B_k^P(\lambda,\bar{T}_k)$	-	Planck function representation of intensity of k^{th} concentric ring of plasma, $\bar{T}_k$ is average temperature of k^{th} ring
BEM	-	Brightness-emissivity method
C_1	-	First radiation constant
C_2	-	Second radiation constant
ε_λ	-	Specific emission coefficient
I_λ^P	-	Intensity of plasma layer
$I_j^P(\lambda)$	-	Intensity of plasma along j^{th} line-of-sight position
I_λ^S	-	Intensity of background source
$I_j^T(\lambda)$	-	Total intensity observed along j^{th} line-of-sight position
κ_λ	-	Line absorption coefficient
$\bar{\kappa}_k(\lambda)$	-	Average absorption coefficient in k^{th} concentric ring of plasma
ℓ_{jk}	-	Chordal length segment present in k^{th} concentric ring along j^{th} line-of-sight position
LTE	-	Local thermodynamic equilibrium
λ	-	Wavelength
S_λ	-	Source function
T_B	-	Brightness temperature
T_e	-	Electron temperature
$\bar{T}_k$	-	Average temperature in k^{th} concentric ring
$T(r)$	-	Temperature profile
r	-	Radius
τ_λ	-	Optical depth
$\tau_j(\lambda)$	-	Optical depth along j^{th} line-of-sight position

VII. PUBLICATIONS GENERATED UNDER GRANT NGL 10-005-089

The following papers and journal publications were given or are accepted for publication.

1. "Spectroscopic Diagnostics of a Uranium Plasma," by R. T. Schneider, Seventeenth Symposium on Spectroscopy, January 8-10, 1969, Gainesville, Florida.
2. "Radiation Transfer Study on a Uranium Plasma," by R. T. Schneider, Fifth Annual Southeastern Seminar on Thermal Sciences, April 21-22, 1969, Gainesville, Florida.
3. "Spectroscopic Measurements on a High Pressure Uranium Arc," by R. T. Schneider, G. R. Shipman and A. G. Randol, III, 20th Annual Mid-American Symposium on Spectroscopy, May 12-15, 1969, Chicago, Illinois.
4. "Temperature Measurement on a Uranium Plasma," by R. T. Schneider, G. R. Shipman and J. M. Mack, 8th National Meeting, Society for Applied Spectroscopy, October 6-10, 1969, Anaheim, California, and Applied Spectroscopy, 23, 671 (1969).
5. "Radiation from a Uranium Plasma," by R. T. Schneider, C. D. Kylstra, A. G. Randol III and M. J. Ohanian, American Nuclear Society 15th Annual Meeting, June 15-19, 1969, Seattle, Washington, and ANS Transactions, 12, 3 (1969).
6. "Measurement of the Emission Coefficient of a Uranium Plasma," by R. T. Schneider, A. G. Randol III, C. D. Kylstra and M. J. Ohanian, American Nuclear Society Winter Meeting, November 30 - December 5, 1969, San Francisco, California, and ANS Transactions 12, 413 (1969).

7. "Experimental Determination of the Boiling Point of Uranium," by A. G. Randol III, R. T. Schneider, and C. D. Kylstra, American Nuclear Society Winter Meeting, November 30 - December 5, 1969, San Francisco, California, and ANS Transactions 12, 541 (1969).

8. "Properties of a Uranium Plasma," by H. D. Campbell, R. T. Schneider and C. D. Kylstra, 8th Aerospace Science Meeting, AIAA, January 19-27, 1970, New York.

9. "Measurement of the Temperature and Partial Pressure of a Uranium Plasma," by R. T. Schneider, G. R. Shipman and A. G. Randol III, Applied Spectroscopy 24, 253-258 (1970).

10. "Experimental Investigations of a Uranium Plasma Pertinent to a Self Sustaining Plasma Source," Annual Report, September 1969.

11. "Boiling Point of Uranium," by A. G. Randol III, R. T. Schneider and C. D. Kylstra, Symposium on Research on Uranium Plasmas and Their Technological Application, January 7-10, 1970, Gainesville, Florida.

12. "Spectroscopic Study of a Uranium Arc Plasma," by H. D. Campbell, R. T. Schneider, C. D. Kylstra and A. G. Randol III, Symposium on Research on Uranium Plasmas and Their Technological Application, January 7-10, 1970, Gainesville, Florida.

13. "Generation of a Fissioning Plasma," by C. D. Kylstra and R. T. Schneider, Symposium on Research on Uranium Plasmas and Their Technological Application, January 7-10, 1970, Gainesville, Florida.

14. "Uranium Plasma Research at the University of Florida," by R. T. Schneider, C. D. Kylstra and M. J. Ohanian, Sixth Intercenter and Contractors Conference on Plasma Physics, December 8-10, 1969, Langley Research Center.

15. "Review of Uranium Plasma Research," by R. T. Schneider, Meeting of the NASA Research and Technology Advisory Subcommittee on Electrophysics, NASA Lewis Research Center, Cleveland, Ohio, April 13-14, 1970.

16. "Uranium Plasma Emission Coefficients," by C. D. Kylstra, R. T. Schneider and H. D. Campbell, AIAA 6th Propulsion Joint Specialist Conference, San Diego, California, June 15-19, 1970.

17. "Experimental Investigations of a Uranium Plasma Pertinent to a Self Sustaining Plasma Source," Annual Report, May 1970.

18. "Plasma Diagnostics of a Uranium Plasma," by R. T. Schneider, C. D. Kylstra and H. D. Campbell, International Conference on Gas Discharges, London, U.K., September 15-18, 1970.

19. "Generation of a Uranium Plasma at Near Gaseous Core Reactor Conditions," by J. F. Davis III, B. G. Schnitzler and R. T. Schneider, 2nd Symposium on Uranium Plasmas: Research and Application, Atlanta, Georgia, November 15-17, 1971.

20. "Ballistic Piston Fissioning Plasma Experiment," by B. E. Miller, K. Thom, R. T. Schneider and G. T. Lalos, 2nd Symposium on Uranium Plasmas: Research and Application, Atlanta, Georgia, November 15-17, 1971.

21. "Excitation and Ionization of a CO_2 Laser by Nuclear Reaction Products," by H. S. Rhoads and R. T. Schneider, Bull. of the Amer. Phys. Soc. (in print).

22. "Plasma Properties of a D.C. Uranium Arc," by J. M. Mack, Jr., J. L. Usher, R. T. Schneider and H. D. Campbell, Bull. of the Amer. Phys. Soc. (in print).

23. "Uranium Plasma Emission Coefficient in the Visible and Near U.V.," J. M. Mack, Jr., J. L. Usher, H. D. Campbell and R. T. Schneider, 2nd Symposium on Uranium Plasmas: Research and Application, Atlanta, Georgia, November 15-17, 1971.

24. "CO_2 Laser Experiments Using Nuclear Reactions as the Ionization Source," by H. S. Rhoads, R. T. Schneider and F. Allario, 2nd Symposium on Uranium Plasmas: Research and Application, Atlanta, Georgia, November 15-17, 1971.

25. "Nuclear Pumped Gas Lasers," by K. Thom and R. T. Schneider, AIAA Journal (in print).

26. "Research on Uranium Plasmas," by K. Thom and R. T. Schneider, NASA SP-236 (1971).

27. "Temperature Profile Determination in an Absorbing Plasma," by J. L. Usher and H. D. Campbell, submitted to JQSRT.

The following dissertations and theses were generated under the program.

1. "A Determination of High Pressure, High Temperature Uranium Plasma Properties," by Arthur G. Randol III, Dissertation, University of Florida, 1969.

2. "Temperature Profile Determination of a Uranium Plasma in a Helium Atmosphere," by J. M. Mack, Jr., Master's Thesis, University of Florida, June 1969.

3. "Temperature Profile Determination in an Absorbing Plasma", by John L. Usher, Master's Thesis, University of Florida, August 1971.

4. "Thermodynamic Study of Rapid Compression of UF_6", by Barry E. Miller, Master's Thesis, University of Florida, November 1971.

5. "Generation of Uranium Plasma with a Sliding Spark," by John F. Davis, Master's Thesis, University of Florida, March 1972 (tentative)

6. "Direct Nuclear Excitation of a CO_2 Laser," by Harold S. Rhoads, Ph.D. Dissertation, University of Florida, January 1972.